THE GEOLOGICAL SOCIETY OF AMERICA®

Structural architecture and composition of crystalline basement offshore west Norway

Antje Lenhart[1,*], Christopher A.-L. Jackson[1], Rebecca E. Bell[1], Oliver B. Duffy[2], Robert L. Gawthorpe[3], and Haakon Fossen[4]

[1]BASINS RESEARCH GROUP (BRG), DEPARTMENT OF EARTH SCIENCE AND ENGINEERING, IMPERIAL COLLEGE, SOUTH KENSINGTON CAMPUS, PRINCE CONSORT ROAD, LONDON, SW7 2BP, UK

[2]BUREAU OF ECONOMIC GEOLOGY, JACKSON SCHOOL OF GEOSCIENCES, THE UNIVERSITY OF TEXAS AT AUSTIN, UNIVERSITY STATION, BOX X, AUSTIN, TEXAS 78713-8924, USA

[3]BASIN AND RESERVOIR RESEARCH GROUP, DEPARTMENT OF EARTH SCIENCE, UNIVERSITY OF BERGEN, ALLÉGATEN 41, 5020 BERGEN, NORWAY

[4]MUSEUM OF NATURAL HISTORY/DEPARTMENT OF EARTH SCIENCE, UNIVERSITY OF BERGEN, ALLÉGATEN 41, POSTBOX 7803, 5007 BERGEN, NORWAY

ABSTRACT

Numerous studies have investigated the geodynamic history and lithological composition of the Proterozoic basement, Caledonian nappes, and Devonian extensional basins and shear zones onshore west Norway. However, the offshore continuation of these structures, into the northern North Sea, where they are suspected to have influenced the structural evolution of the North Sea rift, is largely unknown. Existing interpretations of the offshore continuation of Caledonian and Devonian structures are based on simple map-view correlations between changes in offshore fault patterns and pronounced onshore structures, without providing evidence for the presence, nature, and geometry of offshore, basement-hosted structures.

By integrating three-dimensional (3-D) seismic, borehole, and onshore geological and petrophysical data, as well as two-dimensional (2-D) forward modeling of gravity and magnetic data, we reveal the structural architecture and composition of the crystalline basement on the Måløy Slope, offshore west Norway. Based on 3-D mapping of intrabasement reflection patterns, we identified three basement units that can be correlated with the Caledonian thrust belt, and the major Devonian Nordfjord-Sogn detachment zone, located only 60 km to the east, onshore mainland Norway. Similar to that observed onshore, offshore crystalline basement of the Proterozoic basement (Western Gneiss Region) and allochthons is folded into large-scale antiforms and synforms. These units are separated by the strongly corrugated Nordfjord-Sogn detachment zone. Our analyses show that different types of crystalline basement can be distinguished by their seismic reflection character, and density and magnetic properties. We speculate that the main causes of the observed intrabasement reflectivity are lithological heterogeneities and strain-induced structures such as shear and fracture zones. Our interpretation of the architecture of crystalline basement offshore west Norway has important implications for the location of the suture zone between Baltica and Laurentia.

LITHOSPHERE GSA Data Repository Item 2019086 https://doi.org/10.1130/L668.1

INTRODUCTION

The discovery of hydrocarbon plays related to fractured and weathered crystalline basement (e.g., Nelson, 2001; Cuong and Warren, 2009; Hartz et al., 2013) has driven interest in the nature and three-dimensional (3-D) geometry of intrabasement structures. Furthermore, an increasing number of studies are demonstrating how the composition and structure of crystalline basement can influence the geometry and growth of normal faults developing within overlying cover strata, in addition to the physiography of the associated rift basin (e.g., Morley et al., 2004; Paton, 2006; Morley, 2009, 2010; Kirkpatrick et al., 2013; Phillips et al., 2016). Despite their importance, the geometry and composition of crystalline basement are largely neglected or simply considered homogeneous in analogue and numerical models (e.g., Gupta et al., 1998; Cowie et al., 2000; Huismans and Beaumont, 2008); as such, these properties are not explicitly represented in tectono-stratigraphic models of rift development (e.g., Gawthorpe and Leeder, 2000). A better understanding of basement heterogeneity will, however, allow us to: (1) construct more realistic physical and numerical models of rift tectono-stratigraphic development; (2) understand how basement properties control structural inheritance in a range of tectonic settings (e.g., rifts, orogenic belts); and (3) better account for heat-flow variations and impacts in numerical models of basin geodynamics.

The northern North Sea rift is considered to have formed above a heterogeneous substrate with, in places, structures inherited from previous Proterozoic and Paleozoic contractional and extensional events (e.g., Bartholomew et al., 1993; Færseth et al., 1995; Roberts et al., 1995; Færseth, 1996; Doré et al., 1997; Fossen et al., 2016; Fazlikhani et al., 2017). These structures include strongly deformed Precambrian basement, allochthonous rocks, and large-scale Devonian extensional shear zones and faults that are exposed onshore west Norway, immediately east of the rift (e.g., Andersen and Jamtveit, 1990; Fossen, 1992; Andersen and Andresen, 1994; Milnes et al., 1997; Eide et al., 1997, 1999; Krabbendam and Dewey, 1998; Fossen, 2000; Osmundsen and Andersen, 2001; Johnston et al., 2007). Despite intensive study of the formation and collapse of the Caledonides onshore west Norway, in addition to northern Scotland, Orcadia and West Orkney Basin, and the Greenland Caledonides (e.g., Brewer and Smythe, 1984; McGeary and Warner, 1985; Cheadle et al.,

*antje.lenhart@gmail.com

1987; Coward et al., 1989; Snyder, 1990; Bird et al., 2015; Norton et al., 1987; Coward, 1990; Wilson et al., 2010; Andresen et al., 2007; Gilotti and McClelland, 2008), the onshore geology can be projected offshore for only a short distance, meaning the structural architecture and composition of the crystalline offshore basement remain poorly understood.

Most studies base their interpretation of offshore pre-existing basement structures on widely spaced, relatively low-resolution, two-dimensional (2-D) seismic reflection and potential field data, as well as regional-scale, principally map-view correlations of offshore fault geometries with onshore basement structures, without providing evidence for the nature, location, and geometry of intrabasement structures (e.g., Færseth et al., 1995; Færseth, 1996; Doré et al., 1997; Fossen et al., 2016). Few studies have attempted to decipher the composition and location of intrabasement structures beneath the North Sea rift using geophysical data (e.g., Reeve et al., 2014; Fossen et al., 2016; Phillips et al., 2016; Fazlikhani et al., 2017). Using borehole, gravity, and magnetic data, Smethurst (2000) presented an interpretation of basement lithology and structures offshore west Norway, but the 3-D structural architecture of the crystalline basement remains unclear. Furthermore, due to their inherent ambiguity, gravity and magnetic data alone may lead to false interpretations if not constrained by a sound subsurface model and petrophysical data. Recently, Fazlikhani et al. (2017) showed that the crystalline basement beneath the northern North Sea exhibits a varying seismo-acoustic character that can be divided into three primary seismic facies that can be mapped throughout the basin. Despite this advance, Fazlikhani et al. (2017) only used 2-D seismic reflection data, and they did not constrain their interpretation with other available data (e.g., potential field). Borehole data could support seismic reflection–based interpretations by providing direct constraints on basement composition and, if sufficiently closely spaced, structure. However, many boreholes terminate above crystalline basement, with those that do sample basement being widely spaced. This, combined with poor seismic data resolution, complicates the imaging and interpretation of complex 3-D intrabasement structures.

Intrabasement seismic reflectivity, such as that identified and mapped by Fazlikhani et al. (2017), may be the result of compositional and structural heterogeneities within the crust, and the type and amount of ductile and brittle deformation that an area experienced (e.g., Smythe et al., 1982; Jones and Nur, 1984; Wang et al., 1989; Goff and Holliger, 2003; Smithson and Johnson, 2003; Meissner et al., 2006; Lyngsie et al., 2007; Bongajum et al., 2012; Ahmadi et al., 2016; Hedin et al., 2016). Although intrabasement structures have been described from regional, deep-imaging 2-D seismic reflection profiles (e.g., Wang et al., 1989; Allmendinger et al., 1987; Kern and Wenk, 1990; Reston, 1996; Cook et al., 1999; Abramovitz and Thybo, 2000; Juhojuntti et al., 2001; Simancas et al., 2003; Torvela et al., 2013; Ruiz et al., 2017), few studies use borehole data (e.g., Christensen and Szymanski, 1988; Zhang et al., 2005; Hedin et al., 2012, 2014, 2016; Lorenz et al., 2015), synthetic seismogram modeling (e.g., Fountain et al., 1984; Hurich et al., 1985; Reeve at al., 2014; Phillips et al., 2016; Kennett et al., 2017; Veludo et al., 2017), and/or gravity and magnetic forward modeling (e.g., Ebbing et al., 2006; Lyngsie and Thybo, 2007; Ritzmann and Faleide, 2007; Marello et al., 2010; Gernigon and Brönner, 2012; Lassen and Thybo, 2012; Mazur et al., 2015; Olyphant et al., 2017) to help further constrain a largely seismic reflection–based interpretation.

Determining the sources of crustal reflectivity, and mapping crystalline basement structure and composition require a holistic approach, drawing on a range data types, methods, and scales of observation. On the Måløy Slope, offshore west Norway (Fig. 1A), intrabasement structures are well imaged in seismic reflection data due to relatively shallow burial of the pre-Devonian metamorphic basement beneath a thin (<3.5 km) and stratigraphically simple sedimentary cover (Fig. 2). Due to its complex but well-known tectonic history, which yielded a wide variety of crystalline rock types and associated structures, the study area serves as an ideal natural laboratory in which to constrain the geometry, investigate the origin, and establish the regional importance of intrabasement reflectivity. We used borehole and core data, conventional 2-D and 3-D seismic reflection data, gridded potential field data, and 2-D forward modeling of gravity and magnetic data to constrain the nature, composition, and 3-D architecture of the crystalline basement on the Måløy Slope.

Our results show that intrabasement reflections correlate with major structures and basement units comprising the Proterozoic basement and allochthonous nappes of the Caledonian thrust belt and associated Devonian extensional shear zones. By linking onshore and offshore structures, we can reveal the 3-D geometry of large-scale intrabasement structures along the western part of the Norwegian margin. Using the depth and architecture of these intrabasement structures, we briefly discuss the implications of our interpretation for the highly uncertain location of the suture zone between Baltica and Laurentia. In addition, based on the known geological history, we suggest several plausible origins for intrabasement reflectivity mapped within the study area. We show that the primary causes of basement reflectivity are lithological heterogeneities, and associated interference and scattering effects of the seismic wave field, as well as strain-induced structures such as shear and fracture zones. Based on our results, we consider that the approach followed in this study can be applied in other subsurface studies to help us more confidently interpret the origin of intracrystalline basement reflectivity in other sedimentary basins.

GEOLOGICAL FRAMEWORK

Study Area

The study area is located along the Måløy Slope, offshore west Norway, comprising an area of ~3600 km^2 (Fig. 1A). The western boundary of the study area is defined by the Sogn graben; the southern and northern boundaries are approximately coincident with the coastal outlets of the Sognefjord and Nordfjord, respectively, two major fjords onshore western Norway. Onshore, Proterozoic basement (Western Gneiss Region [WGR]), remnants of the Caledonian thrust belt, a major Devonian extensional shear zone, and several intermontane Devonian sedimentary basins are preserved (e.g., Andersen and Andresen, 1994; Milnes et al., 1997; Johnston et al., 2007, Vetti and Fossen, 2012). These basement units are suspected to form the metamorphic, crystalline basement offshore west Norway (e.g., Smethurst, 2000; Reeve et al., 2014), but their offshore continuation and 3-D geometry remain unclear (Færseth et al., 1995; Smethurst, 2000).

Regional Tectonic History

The crystalline basement in the northeastern North Sea is largely the result of terrane accretion during the Sveconorwegian and Caledonian orogenies (Ziegler, 1975; Fossen, 1992; Bingen et al., 2008; Gee et al., 2008). The Caledonian orogeny culminated in SE-directed thrusting of allochthonous and parautochthonous nappes onto the subducting margin of Baltica, which is commonly termed the Western Gneiss Region (WGR; ca. 403 Ma; Andersen et al., 1991; Fossen, 1992; Fossen and Dunlap, 1998; Root et al., 2004; Gee et al., 2008). Early to Middle Devonian postorogenic extension (ca. 400 Ma) resulted in W- to WNW-directed backsliding of the nappe pile along a reactivated low-angle Caledonian décollement zone (Fossen, 1992, 2000; Fossen and Dunlap, 1998), the formation of large-scale WNW-dipping extensional shear zones (Nordfjord-Sogn detachment zone [NSDZ]), exhumation of the WGR, and the formation of Devonian continental basins (Andersen, 1998; Fossen,

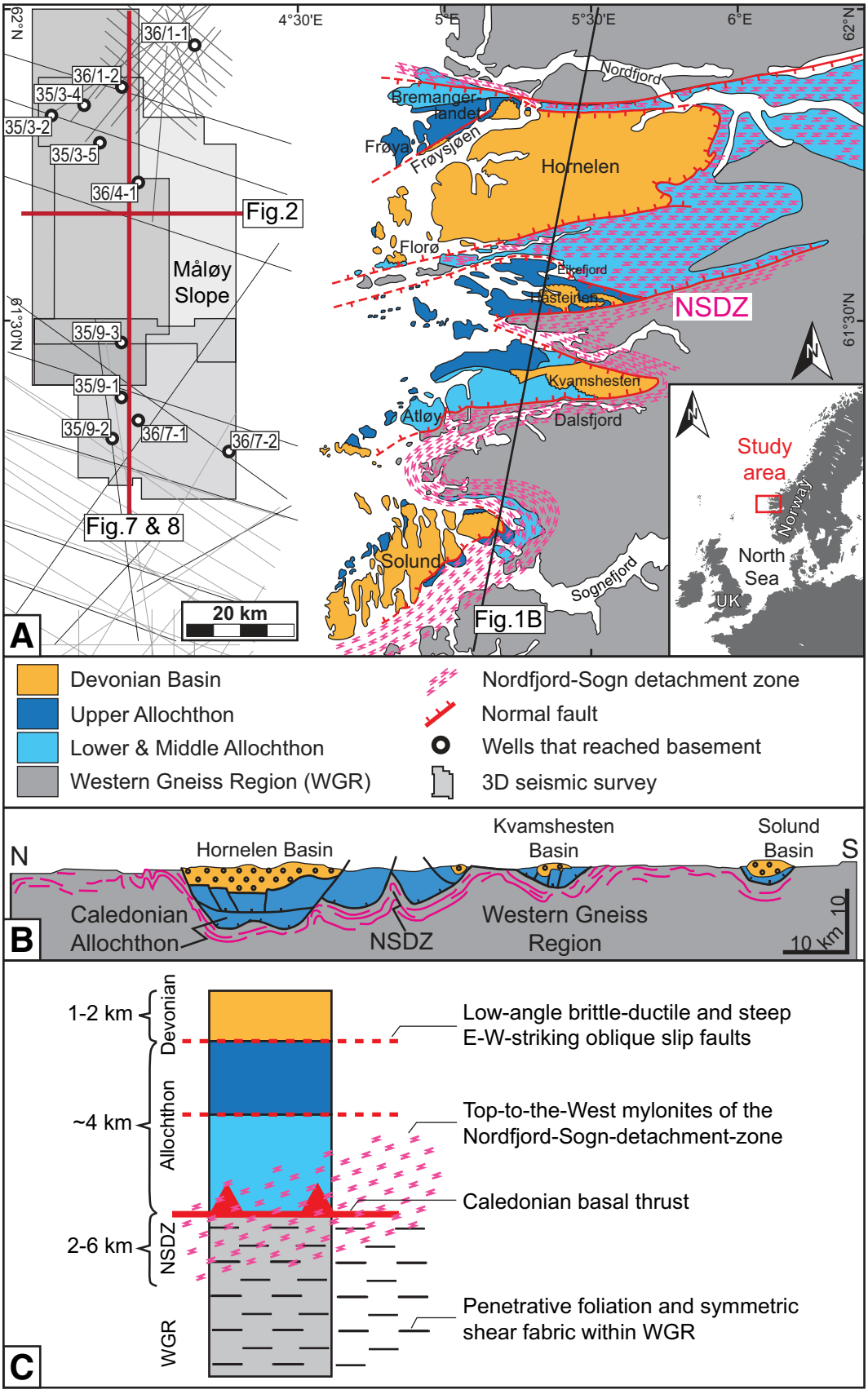

Figure 1. (A) Location of study area, offshore two- and three-dimensional (3D) seismic reflection surveys, and boreholes. Onshore geology is based on Andersen and Jamtveit (1990). (B) Schematic N-S cross section through the onshore part of the study area taken from Osmundsen and Andersen (2001) showing the large-scale folded architecture of the crystalline basement. The Western Gneiss Region (WGR) crops out in the antiforms, whereas allochthons and Devonian basins are preserved in the synforms; the Nordfjord-Sogn detachment zone (NSDZ) separates the WGR from allochthonous rocks. (C) Tectono-stratigraphic setting of the crystalline basement onshore west Norway based on Johnston et al. (2007). Note that the NSDZ is imprinted on the WGR and Lower and Middle Allochthons.

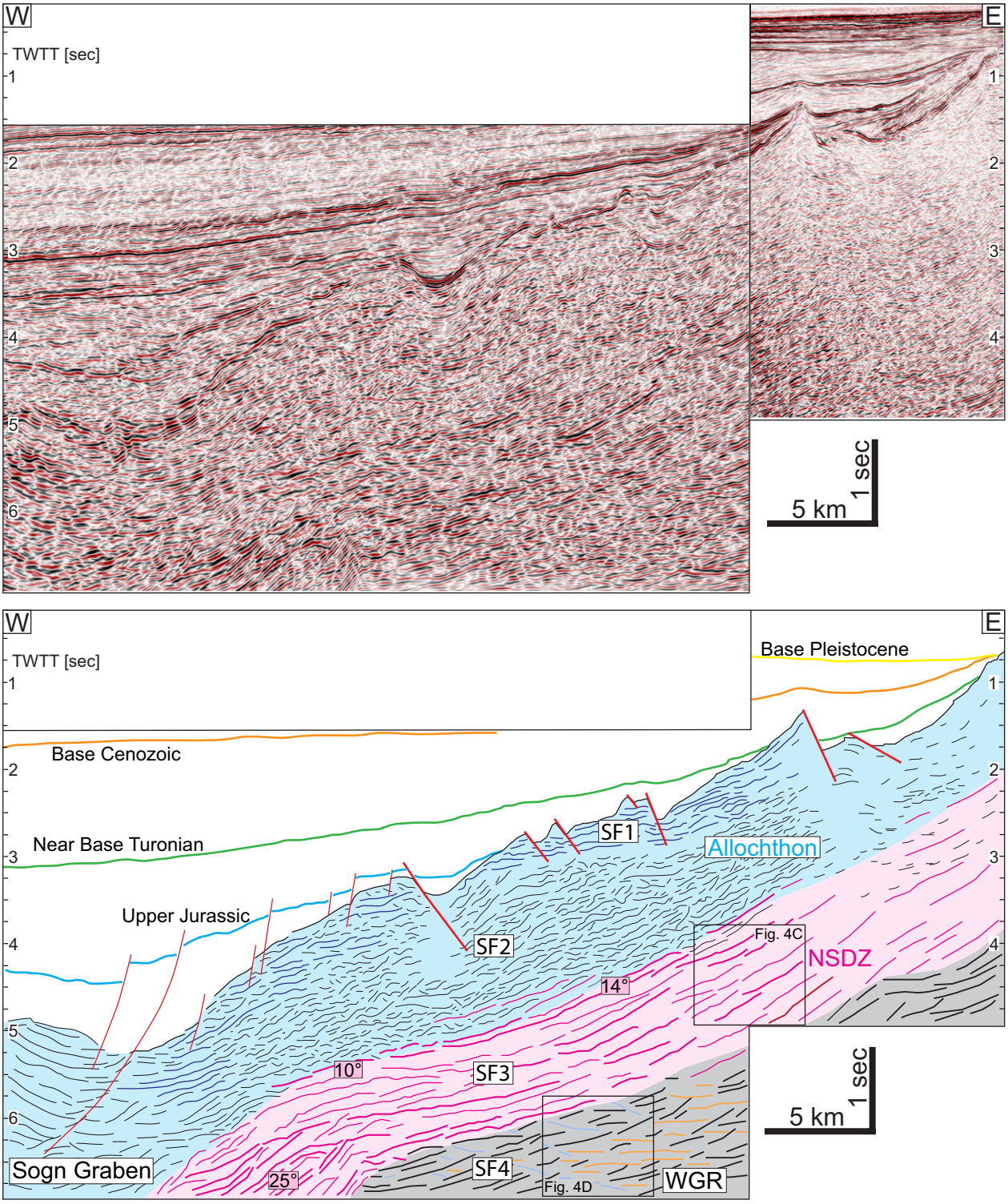

Figure 2. Uninterpreted and interpreted E-W–trending seismic section showing the seismic expression of crystalline basement along the Måløy Slope. Identified and interpreted intrabasement seismic facies (SF1–SF4) and average dip angles of intrabasement reflections and reflection packets are indicated. Colors correspond to tectono-stratigraphic units shown in Figure 1C. See Figure 1A for location. TWTT—two-way traveltime; NSDZ—Nordfjord-Sogn detachment zone; WGR—Western Gneiss Region.

2000; Osmundsen and Andersen, 2001). Simultaneously, N-S shortening, related to the interplay of the NSDZ and left-lateral movement along the Møre-Trøndelag fault complex (MTFC) further north, resulted in transtensional folding of the WGR, the detachment zone, and the Caledonian allochthons and Devonian deposits (Chauvet and Séranne, 1994; Krabbendam and Dewey, 1998; Dewey and Strachan, 2003; Osmundsen and Andersen, 2001; Fossen et al., 2013). Offshore, crystalline basement along the Måløy Slope is displaced by Middle to Late Jurassic normal faults and is unconformably overlain by Mesozoic strata (e.g., Færseth et al., 1995; Sømme et al., 2013; Reeve et al., 2015).

Onshore Geological Framework and Basement Units

The WGR is located in the footwall of the NSDZ (Figs. 1C and 2) and is composed of highly deformed Proterozoic (1750–900 Ma; Engvik and Andersen, 2000) granodioritic and migmatitic gneisses, and strongly foliated amphibolites, augen-gneisses, and anorthosites (Hacker et al., 2010). Meter- to kilometer-scale, E-W–elongated lenses of granulites, gabbros, and eclogite bodies are common. Devonian extension and exhumation of the WGR strongly reworked and obliterated many Caledonian structures, with the associated rock foliation being generally subparallel to the NSDZ, following gently W-plunging, WGR-cored antiforms and synforms (Dewey et al., 1993).

The allochthonous nappe stack is located in the hanging wall of the NSDZ and is further divided into the Lower, Middle, and Upper Allochthons (Fig. 1; Roffeis and Corfu, 2014). The Lower Allochthon consists of gneisses and weakly metamorphosed sandstones and graywackes of the Baltica craton (Hacker and Gans, 2005; Johnston et al., 2007). The Middle Allochthon is characterized by orthogneisses, granulites, gabbros, and anorthosites, which formed the basement and cover sequences of the western Baltica margin (Andersen et al., 1994; Krabbendam et al., 2000). The Upper Allochthon is composed of ophiolitic and island-arc–derived material that is exotic to Baltica (Andersen et al., 1994; Johnston et al., 2007). The total thickness of the allochthons is highly variable, but their minimum present-day thickness is estimated to be ~4 km (Johnston et al., 2007).

The rocks of the allochthons are unconformably overlain by Devonian metasediments of the Hornelen, Håsteinen, Kvamshesten, and Solund basins (Fig. 1; Osmundsen and Andersen, 2001). The Devonian metasediments generally comprise basin margin–attached, upward-coarsening packages of alluvial-fan sandstones and conglomerates of allochthonous provenance (Cuthbert, 1991; Osmundsen and Andersen, 2001; Templeton, 2015). In the basin axes, upward-coarsening, up to 200-m-thick, alluvial plain and lacustrine successions occur (Steel, 1976; Steel et al., 1977; Steel and Aasheim, 1977). The Devonian deposits experienced anchizone to lower-greenschist-facies metamorphism (Seranne and Seguret, 1987; Torsvik et al., 1986; Sturt and Braathen, 2001), corresponding to sediment burial depths of 5–13 km (Svensen et al., 2001) and maximum temperatures of 300 °C (±50 °C).

The NSDZ is the principal shear zone in the study area. This structure formed to accommodate Devonian extensional tectonics and associated exhumation of the WGR (e.g., Fossen, 2000). The NSDZ juxtaposes high-pressure rocks of the WGR in its footwall against low-grade metamorphic rocks of the allochthons and Devonian basins in its hanging wall (Fig. 1C). The shear zone is folded into a series of kilometer-scale, E-W–trending antiforms and synforms that plunge to the west with varying dips (~5°–25° to W-WNW; Fig. 1C; Norton, 1987; Labrousse et al., 2002). The 2–6-km-thick (Norton, 1986, 1987; Johnston et al., 2007), W-dipping NSDZ is composed of various mylonitic rock types that indicate varying degrees of deformation under retrograde amphibolite- to greenschist-facies conditions; these rock types imply that the detachment initially formed at crustal depths between 20 km (Wilks and Cuthbert, 1994) and 30–40 km (Johnston et al., 2007).

DATA SETS AND METHODS

Borehole, Core, and Petrophysical Data

Onshore and offshore core, borehole, and petrophysical data were used to constrain the composition and physical properties of crystalline rocks along the Måløy Slope. Eleven offshore boreholes penetrate crystalline basement (Norwegian Petroleum Directorate [NPD] Web site: www.npd.no/en/Topics/Wells/; Knape, 1996; Fig. 1A), with three providing cores extracted from crystalline basement rock; we analyzed these cores for basement mineral composition and rock type (Fig. 3; Table 1). Using publicly available well reports, we compiled detailed information about different basement lithologies present offshore west Norway (Table 1). In addition, we collated petrological and petrophysical data for various rock types within each basement unit onshore west Norway from literature (Skjerlie, 1985; Norton, 1986; Dewey et al., 1993; Andersen et al., 1994; Osmundsen and Andersen, 1994; Osmundsen et al., 1998; Bryhni and Lutro, 2000a, 2000b; Lutro and Bryhni, 2000; Krabbendam et al., 2000; Ebbing et al., 2006; Slagstad et al., 2008; Vetti, 2008; Olesen et al., 2010; Reynisson et al., 2010; Hedin et al., 2014), and we screened ~1200 published onshore rock samples and seven boreholes for rock type, geological unit, density, and susceptibility (NGU database, http://aps.ngu.no/kart/geofysikk/; Table 2). Mean values and standard deviations of density and susceptibility were calculated for the 20 most common and statistically significant onshore rock types (Table 2). These density and susceptibility data provided important constraints for our assessment of the basement composition, and the 2-D forward modeling of gravity and magnetic data drawing on these data.

Seismic Reflection Data

The study area is covered by 2-D seismic reflection profiles (imaging to 7–9 s two-way traveltime [TWT]), and four partly overlapping, post-stack time-migrated 3-D seismic surveys of moderate to good quality (imaging to 5–7 s TWT; Fig. 1A). These data were processed in zero-phase and are presented in reversed polarity as adopted by the Society of Exploration Geophysicists (SEG) convention, where red colors (trough) indicate a downward increase in acoustic impedance. The dominant frequency within intrabasement reflections, extracted from the 3-D seismic data, ranges from 10 to 30 Hz. To improve the signal-to-noise ratio, 3-D seismic volumes were frequency filtered to reduce coherent and random noise (for details about the noise filtering process, see GSA Data Repository Item DR1[1]). To estimate the true depth and geometry of basement structures, seismic data were depth converted using a 3-D velocity model (see Data Repository Item DR2). The top of the crystalline basement, directly tied to well data, is characterized by a high-amplitude trough-peak reflection event (e.g., Fig. 2). Seismic interpretation within crystalline basement was based on the mapping of individual continuous

[1]GSA Data Repository Item 2019086, Item DR1: Details about the noise-filtering process applied to seismic data; Item DR2: 3-D velocity model and depth conversion of seismic data; Item DR3: Details about the 2-D forward modeling of gravity and magnetic data and figures illustrating several steps of the modelling process; Item DR4: Uncertainties of 2-D forward modelling process; Item DR5: Large-scale version of seismic profile shown in Figure 7; Item DR6: Additional core photos of crystalline basement rocks and locations of cores relative to magnetic anomalies, is available at http://www.geosociety.org/datarepository/2019, or on request from editing@geosociety.org.

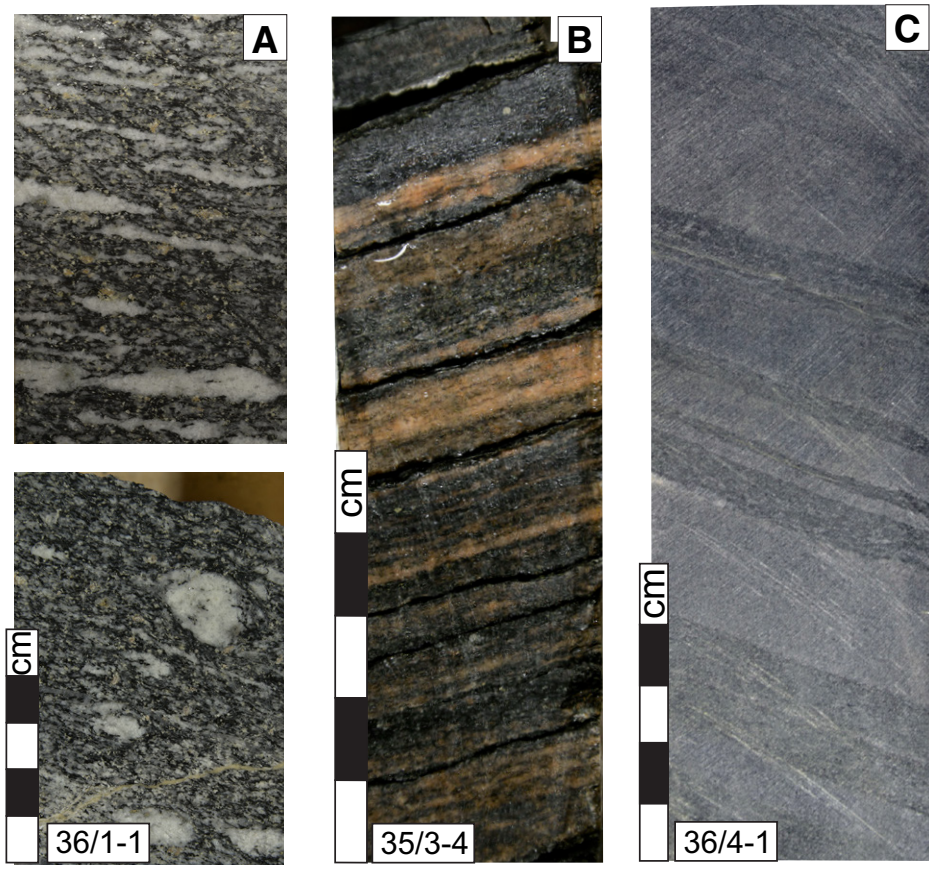

Figure 3. Photographs of crystalline basement cores recovered from boreholes 36/1–1, 35/3–4, and 36/4–1. See Figure 1A for location. (A) Biotite augen gneiss interpreted to be associated with the Western Gneiss Region (WGR). (B) Banded K-feldspar biotite gneiss interpreted to be part of the Lower or Middle Allochthons. (C) Banded biotite gneiss interpreted to belong to either the Lower or Middle Allochthon.

TABLE 1. SUMMARY OF BOREHOLES THAT PENETRATE CRYSTALLINE BASEMENT ALONG THE MÅLØY SLOPE AND INTERPRETATION OF BASEMENT LITHOLOGIES BASED ON CORE DATA

Well	Penetrated basement depth (m)	Core/length (m)	Description from well report	Core description (this study)	Suspected unit
35/3-2	233	No	Mica schist, gneiss (Caledonian?); foliated rock with alternating mica-rich and quartz-feldspar–rich bands; muscovite, chlorite, biotite, epidote; some fractures are filled with secondary calcite; minor amounts of garnet, apatite, and opaque minerals		(Upper) Allochthon
35/3-4	20	Yes; 1.8	Green mica schist, gneiss (Caledonian?); foliated rock with alternating mica-rich and minor quartz-feldspar–rich bands; chlorite, muscovite, biotite, epidote	K-feldspar biotite gneiss (mylonitic)	Middle Allochthon
35/3-5	22	No	Green mica schist, gneiss; foliated, banded, friable; muscovite, chlorite, biotite; quartz bands and minor amounts of calcite		Middle Allochthon
35/9-1	36	No	Greenschist and gneiss; possibly weathered; striated and foliated bands; chlorite, quartz, feldspar, muscovite, biotite, pyroxene/amphibole?, talc/serpentine		Upper Allochthon
35/9-2	29	No	Greenschist and gneiss (Caledonian?); quartz, chlorite, muscovite, garnet, feldspar		Upper Allochthon
35/9-3	13	No	No information available		–
36/1-1	28	Yes; 1	Quartz augen gneiss (Devonian?); weathered top; lense-shaped augens of quartz in groundmass of biotite and K-feldspar; occasionally fractured	Biotite augen gneiss	Western Gneiss Region (WGR)
36/1-2	22.6	No	Garnetiferous quartz-feldspar-epidote schist, gneiss; weak foliation of muscovite and green biotite; frequent occurrence of clinozoisite		Upper Allochthon
36/4-1	5	Yes; 0.4	Greenschist; very hard to blocky, splintery; biotite, chlorite, quartz, plagioclase, calcite	(Dioritic) Banded gneiss	Middle Allochthon
36/7-1	7	No	Gneiss (Precambrian?); angular-splintery quartz, feldspar; traces of muscovite, chlorite, jasper, pyrite, and calcite		WGR
36/7-2	6	No	No information available		–

TABLE 2. AVERAGE DENSITY AND SUSCEPTIBILITY VALUES FOR COMMON BASEMENT ROCK TYPES ONSHORE WEST NORWAY

	Density [g/cm³]				Susceptibility [SI]			
Basement Unit	mean distribution 2.6 3 3.4	Min	Mean	Max	mean distribution 0 0.01 0.02	Min	Mean	Max
Devonian Sediments:								
- Sandstone		2.52	2.72	2.81		0.000028	0.00056	0.0053
- Conglomerate		2.63	2.77	3.07		0.000055	0.0025	0.013
- Conglomerate, Solund		2.75	2.83	2.95		0.00037	0.004	0.0088
- Greywacke		2.65	2.76	3.01		0.00006	0.00095	0.0052
Allochthons:								
- Mica-Schist		2.63	2.8	3.1		0.00009	0.0041	0.036
- Greenschist		2.7	2.89	3.08		0.00023	0.012	0.22
- Phyllite		2.74	2.77	2.8		0.00037	0.00089	0.0028
- Gabbro		2.7	2.93	3.1		0.0003	0.0016	0.0098
- Quartzdiorite		2.65	2.68	2.79		0.00004	0.00012	0.00045
- Quartzite		2.59	2.66	2.8		0.00001	0.00045	0.01
Western Gneiss Region:								
- Granite		2.57	2.65	2.73		0.00012	0.01	0.028
- Granitic Gneiss		2.6	2.65	2.85		0.00005	0.019	0.4
- Granodioritic Gneiss		2.64	2.67	2.82		0.00019	0.024	0.29
- Gneiss		2.56	2.73	3.35		0.00003	0.0075	0.28
- Mica-Gneiss		2.63	2.75	3.04		0.000085	0.0053	0.05
- Banded Gneiss		2.55	2.7	3.02		0.00018	0.0056	0.029
- Augen-Gneiss		2.55	2.68	2.97		0.00007	0.0.01	0.075
- High-pressure Gneiss		2.62	2.93	3.46		0.000099	0.0089	0.093
- Amphibolite		2.7	2.97	3.72		0.000001	0.017	0.6
- Eclogite		2.72	3.31	3.72		0.00006	0.0045	0.047

intrabasement reflections, broader changes in seismic facies, and distinct geometrical relationships (e.g., boundaries) between seismic reflection patterns. To assess whether the observed basement reflectivity is real, and to largely rule out seismic artifacts, we inspected the data for possible multiples, diffractions, and migration artifacts, and we compared the acoustic character of identical structures imaged by different overlapping seismic data sets.

2-D Forward Modeling of Gravity and Magnetic Data

We analyzed gridded Bouguer gravity and aeromagnetic data, and we undertook 2-D forward modeling of gravity and magnetic data to assess the physical properties, and thus likely composition, age, and spatial distribution, of basement rocks along the Måløy Slope. The Bouguer gravity and aeromagnetic data presented in this study (Fig. 6) were extracted from data compiled by the Norwegian Geological Survey (NGU; Skilbrei et al., 2000; Olesen et al., 2010) and have a grid resolution of 500 m. Aeromagnetic data were reduced-to-the-pole using the International Geomagnetic Reference Field (IGRF). The 2-D forward modeling was conducted in the depth-domain in association with the depth-converted interpretation of a seismic line (Fig. 7) located along the model profile; this seismic line provided geometrical constraints on the size and position of modeled basement bodies. We varied density and magnetic properties along the modeled line within the range of known values for each basement rock type onshore (Table 2). Using results from gravity and magnetic data analysis (Olesen et al., 2010; Ebbing et al., 2012), in addition to seismic tomography and refraction profiling studies (Stratford et al., 2009; Stratford and Thybo, 2011; Maupin et al., 2013; Mjelde et al., 2016; Kvarven et al., 2016) from onshore and offshore mid-Norway, we set the depth, density, and susceptibility of the lower crust and mantle to constant values of 23 km, 2.95 g/cm^3, and 0.01 SI, and 30 km, 3.3 g/cm^3, and 0 SI, respectively. To avoid a level of model complexity that we could not constrain with our observations from seismic and onshore geological data, we deliberately chose a simplified modeling approach that assumed no changes in the topography or physical properties of lower-crustal and mantle rocks along our 135-km-long model profile. As a result, our model represents admittedly one of several plausible solutions that could explain the origin and properties of upper-crustal gravity and magnetic signatures, which we here argue readily relate to our understanding of the crystalline basement geology onshore western Norway.

Average densities for Mesozoic and Cenozoic sediments offshore were derived from well-log data from 12 boreholes; we kept these values constant in each model. Additional details about the modeling procedure and its uncertainties are summarized in Data Repository Items DR3 and DR4.

COMPOSITION OF THE CRYSTALLINE BASEMENT

Publicly available data for basement-penetrating wells along the Måløy Slope (Table 1) suggest that the crystalline basement is mainly composed of pre-Devonian gneisses and greenschists/mica schists. In borehole 36/1–1 (Fig. 3A), we describe the basement as a biotite augen gneiss, a rock type typifying the WGR onshore (Hacker et al., 2010). Cores from boreholes 35/3–4 and 36/4–1 (Figs. 3B and 3C) recovered banded gneiss, which is characterized by dipping, millimeter- to centimeter-scale, alternating bands of lighter, feldspar and quartz-rich bands, and darker, biotite-rich bands. Banded or mylonitic gneisses signify pronounced ductile deformation, which is widespread within both the WGR and allochthons. However, based on the mineral composition, and geographical (i.e., offshore Bremangerlandet; Fig. 1) and stratigraphic position of the wells relative to the onshore geology, we infer that boreholes 35/3–4 and 36/4–1 most likely penetrated basement related to the Lower or Middle Allochthon.

With a penetration depth of 233 m, borehole 35/3–2 is the longest drilled section of crystalline basement within the study area and therefore provides important insights into the basement compositional heterogeneity. The crystalline basement is reported to consist of foliated mica schist and gneiss (Table 1); alternating mica-rich and quartz-feldspar–rich bands likely indicate a metamorphic texture similar to the cores from 35/3–4 and 36/4–1 (Figs. 3B and 3C). Furthermore, published well logs show pronounced fluctuations of the P-wave velocity and resistivity values in the uppermost 30 m of the basement. These fluctuations, together with increased neutron values, may indicate that the upper part of the crystalline basement is likely weathered and has fluid-filled fractures

(Bartetzko et al., 2005; NPD Web site: www.npd.no/en/Topics/Wells/). Based on these observations, the rock types in borehole 35/3–2 appear comparable to the banded, mylonitic gneisses drilled in wells 35/3–4 and 36/4–1 (Figs. 3B and 3C) and, hence, are most likely part of the Lower or Middle Allochthon.

SEISMIC REFLECTION CHARACTER OF CRYSTALLINE BASEMENT

Basement Seismic Facies

Based on analysis of reflection continuity, amplitude character, and geometrical relationships between individual reflections and reflection packets, we identified four distinct seismic facies (SF1–SF4) and three common styles of seismic facies relationships (SFRa, SFRb, and SFRc; Figs. 4 and 5). The seismic character, 3-D geometry, and crustal position of each intrabasement seismic facies and seismic facies relationship allowed for a direct correlation with the main basement units exposed onshore. The characteristics of our identified intrabasement seismic facies are similar to the ones described in Fazlikhani et al. (2017), suggesting that the acoustic properties of different parts of the crystalline basement are similar throughout the basin and relatively independent of the properties of seismic reflection data. We here emphasize that amplitude strength may not be directly indicative of rock type, as the seismic data of different vintages processed by different companies will have different automatic gain control applied. Furthermore, an attempt to differentiate seismic facies based on their frequency character was largely inconclusive due to strong frequency variations throughout the interpreted crystalline basement, and unknown data seismic acquisition and processing parameters. Nonetheless, we infer that locally observed higher-frequency seismic facies at depth likely represent rock types characterized by a higher P-wave velocity than the surrounding rocks (e.g., Yilmaz, 1987).

Seismic Facies Analysis

Seismic facies SF1 is characterized by moderately continuous, subparallel, medium- to high-amplitude reflections (Fig. 4A). This reflection pattern is reminiscent of that typically characterizing layered sedimentary successions, which, together with its stratigraphic position in the uppermost part of the basement (Fig. 7), suggests SF1 may represent sedimentary sequences within Devonian metasedimentary rocks. Coarsening-upward cycles within the Devonian basins onshore are locally within the range of seismic resolution (50–200 m; Steel, 1976; Steel et al., 1977; Steel and Aasheim, 1977). Devonian metasediments, however, are not penetrated and thus are not confirmed by any of the offshore wells. An alternative interpretation of the observed reflectivity is that it represents compositional layering within allochthon-related metamorphic rocks.

Seismic facies SF2 consists of both low-amplitude chaotic, and medium- to high-amplitude folded and discontinuous seismic reflections (Fig. 4B), suggesting strongly deformed material. The observed folds exhibit an upright geometry, wavelengths of 2–5 km, and amplitudes of up to hundreds of meters. Based on its crustal position, correlation with well and core data (Fig. 7), and geometric similarity to structures (i.e., folds) observed in the allochthons onshore (e.g., Andersen and Jamtveit, 1990; Osmundsen and Andersen, 1994; Bryhni and Lutro, 2000b), SF2 is suspected to represent rocks of the allochthonous nappes.

Seismic facies SF3 is characterized by a 2–4-km-thick, W-dipping zone of moderately continuous, subparallel, high-amplitude reflections that are defined by high-amplitude trough-peak-trough wave trains (Fig. 4C). The frequency within SF3 seems to be generally higher than in other seismic facies, suggesting the presence of a higher-velocity rock type. Analogous seismic facies are commonly described in deep seismic reflection studies, where they are interpreted as mylonites within ductile shear zones (e.g., Wang et al., 1989; Fountain et al., 1984; Shaocheng et al., 1993; Reeve et al., 2014; Hedin et al., 2014, 2016; Phillips et al., 2016). Mylonites have average P-wave velocities of 6.9 km/s (e.g., Ji et al., 1993; Law and Snyder, 1997), explaining the observed high-frequency character. We therefore interpret SF3 in a similar way, as a thick zone of mylonites.

SF4 is defined by discontinuous, oppositely dipping, high- to very high-amplitude reflections that crosscut or terminate against each other (Fig. 4D). This seismic facies is only observed in the deepest seismically imaged parts of the basement (>12 km deep). Similar seismic facies are described from midcrustal levels within the Paleoproterozoic orogenic belt in southern Finland, where they are interpreted as kilometer-scale, conjugate S-C structures that form a penetrative fabric (Torvela et al., 2013). Andersen and Jamtveit (1990), Dewey et al. (1993), and Osmundsen and Andersen (1994) also described S-C deformation fabrics within the WGR onshore, with these fabrics becoming more common upward toward the NSDZ. We therefore interpret SF4 to represent a large-scale ductile deformation fabric within the WGR.

Seismic Facies Relationships

Abrupt terminations of reflections, and sudden changes from one seismic facies to the other are interpreted as boundaries between different basement units; we used these spatial relationships to reconstruct the 3-D geometry and structural architecture of the crystalline basement (Fig. 5). Unit boundaries are defined by steeply dipping, nonreflective planes that are interpreted as brittle faults (SFRa; Fig. 5A), or by a distinct change in the overall geometry and dip direction between two seismic facies (SFRb; Fig. 5B). The latter boundary type is exclusively associated with SF3 where it is overlain by SF2 above or underlain by SF4. Since we suspect SF3 to represent mylonites, we interpret this contact as a shear contact. A third type of seismic facies relationship was identified across an ~10-km-wide zone in the central part of the study area (SFRc; Figs. 5C and 7). Here, subhorizontal, medium-amplitude reflections of SF1 are crosscut and in parts slightly offset by steeply S- to SW-dipping, high-amplitude reflections that are similar to SF3. Furthermore, the position of the steeply dipping reflections can be linked to small-scale normal faulting at top basement level. Hence, we infer that the zone where we observe SFRc (Fig. 7) comprises an area of intense deformation, i.e., a shear or fracture zone.

GRAVITY AND MAGNETIC SIGNATURE OF CRYSTALLINE BASEMENT

To support our borehole and seismic reflection–based interpretation of the structural architecture and composition of crystalline basement offshore west Norway, we used density and magnetic susceptibility data for the most common onshore basement rock types (Table 2), as well as offshore Bouguer gravity and aeromagnetic data (Fig. 6).

The density and magnetic susceptibility data compiled in Table 2 indicate that Devonian metasediments and rocks of the allochthons and WGR have similar mean densities. The WGR can, however, be distinguished from allochthons and Devonian strata by its strong magnetic character (Table 2). Furthermore, Devonian sediments exhibit very similar magnetic properties to their allochthonous source rocks; these two units may thus be indistinguishable in gravity and magnetic data (Table 2).

Figure 6 shows gridded Bouguer gravity and aeromagnetic data covering the offshore part of the study area. Two positive gravity anomalies are observed: (1) a pronounced N-trending, positive gravity high (maximum 50 mGal) extending along the coastline of west Norway (anomaly A1),

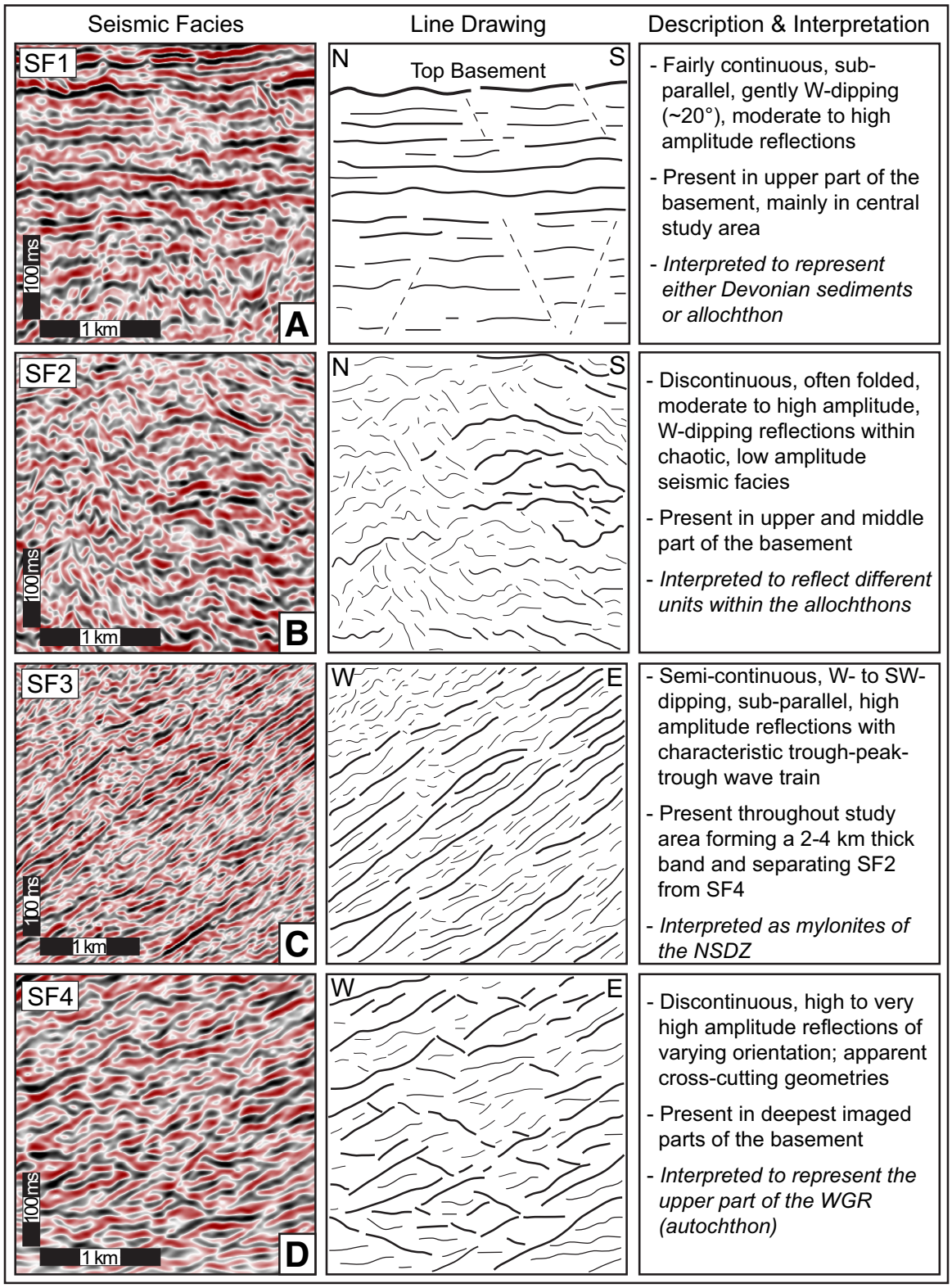

Figure 4. Seismic character, line drawing, and interpretation of intracrystalline basement seismic facies (SF1–SF4) identified in three-dimensional (3-D) seismic data along the Måløy Slope. NSDZ—Nordfjord-Sogn detachment zone; WGR—Western Gneiss Region.

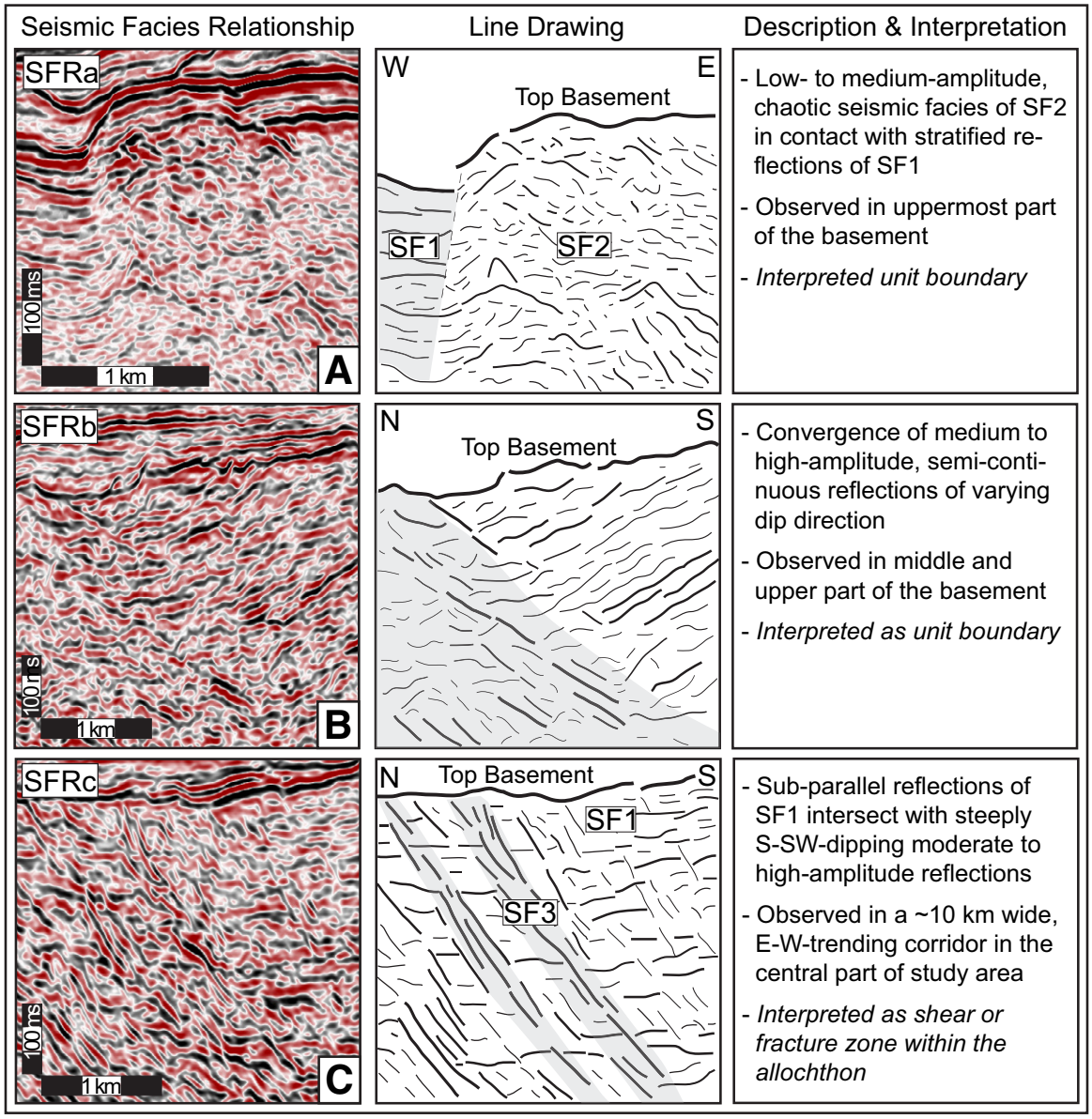

Figure 5. Seismic character, line drawing, and interpretation of geometrical relationships between different seismic facies relationships (SFRa, SFRb, SFRc). SF1–SF4—seismic facies 1–4.

and (2) a WSW-trending, positive anomaly with maximum values of 34 mGal (anomaly A2) located west of Dalsfjord (Fig. 6A). Anomaly A2 is further characterized by a strong, short-wavelength positive magnetic anomaly (155 nT) indicating a dense and magnetic source body at relatively shallow depth (Fig. 6B). According to completion reports, boreholes 36/7–1 and 35/9–1, which are located above the anomaly, drilled through granitic gneiss (typical for WGR; Hacker et al., 2010) and greenschist/gneiss (typical for allochthon; Andersen et al., 1994; Johnston et al., 2007), respectively (Table 1). Based on its position along strike of large-scale, WGR-cored antiforms observed onshore (Osmundsen and Andersen, 2001; Fig. 1B), and the folded reflections observed in seismic data (Fig. 7), we interpret anomaly A2 as a WSW-plunging WGR-cored antiform. The high gravity values of anomaly A1 point to a dense, shallow source body; with basement rocks being exposed on the islands offshore west Norway, it seems logical that anomaly A1 represents a crystalline basement high sub-cropping the seafloor. The steep, W-dipping gradients along the western boundary of anomaly A1 may be caused by a strong lateral density contrast between the crystalline basement-cored high in the east and Mesozoic and Cenozoic marine sediments in the west, the effect of which is enhanced by a N-S–striking, W-dipping, basin-bounding fault (fault Øygarden 2 in Bell et al., 2014; see also Fig. 6A).

A pronounced ENE-trending, ~4-km-wide, linear positive magnetic anomaly (165 nT; anomaly A3; Fig. 6B) around the islands of the Florø area is located along strike of the broadly ENE-WSW–striking Haukå fault (HF) and Eikefjord fault (EF), which bound a gneissose, WGR-cored horst (Lutro and Bryhni, 2000). Magnetic anomaly A4 is located 20 km north of the Florø horst, SW of Bremangerlandet, and it is suspected to be associated with a gabbronoritic/dioritic intrusion that has been described from the island of Frøya (443 ± 4 Ma old Gåsøy intrusion; Hansen et al., 2002; see also Fig. 6B).

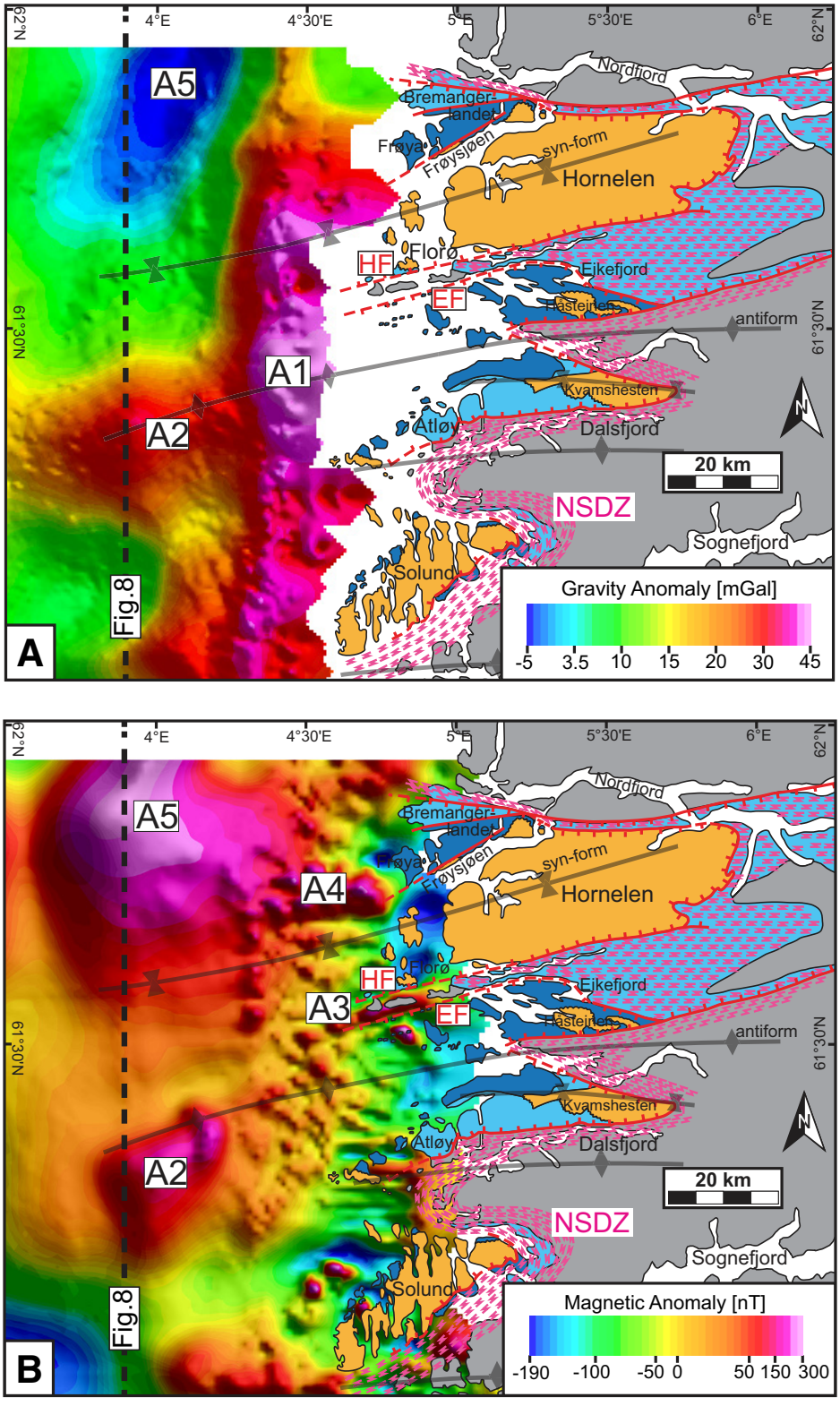

Figure 6. (A) Bouguer gravity anomaly map (illumination direction: 45° declination, 45° inclination) and (B) aeromagnetic anomaly map (illumination direction: 75° declination, 85° inclination) in relation to the onshore geology and major basement synforms and antiforms. Anomalies described in the text are labeled. HF—Hauká fault; EF—Eikefjord fault; NSDZ—Nordfjord-Sogn detachment zone. The location of the N-trending profile used for two-dimensional forward modeling of gravity and magnetic data is indicated. Colors are illustrated using an equal-area color scale ("histogram equalization") to enhance the contrast between low and high anomalies.

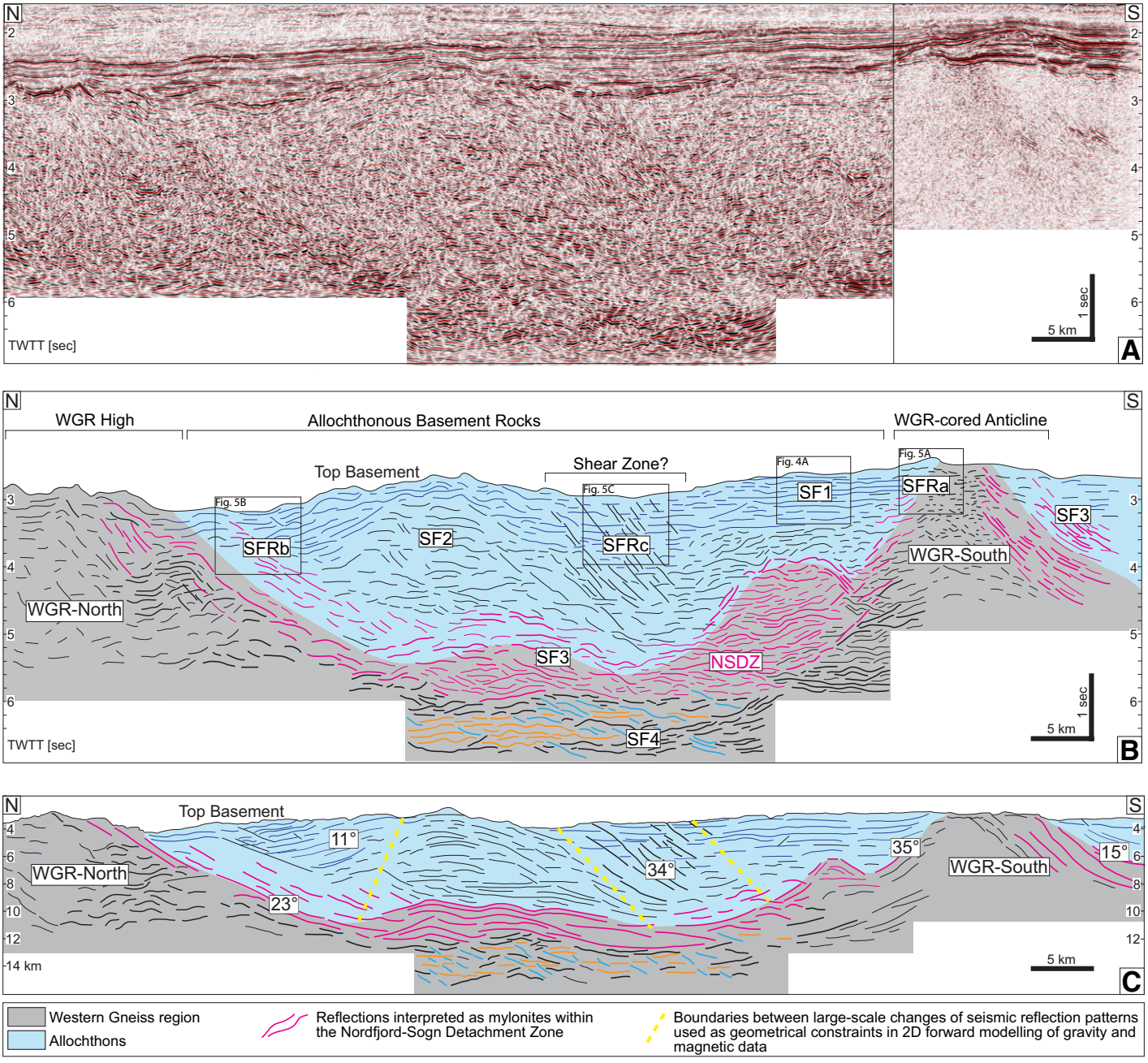

Figure 7. (A) Uninterpreted, (B) interpreted, and (C) depth-converted (scale 1:1) seismic section showing the structural architecture of crystalline basement along the Måløy Slope. Seismic facies and seismic facies relationships are indicated. Colors correspond to tectono-stratigraphic units shown in Figure 1C. The crystalline basement is interpreted to be composed of large Western Gneiss Region (WGR)–cored antiforms with allochthonous material in synforms. These structures can be correlated along strike with basement antiforms and synforms onshore as well as with distinct positive magnetic anomalies (Fig. 6). The Nordfjord-Sogn detachment zone (NSDZ) can be mapped as a 2–4-km-thick band of high-amplitude, moderately continuous reflections that follow the folded architecture of the WGR. See Figure 1A for location. TWTT—two-way traveltime; SFRa, SFRb, SFRc—seismic facies relationships; SF1–SF4—seismic facies 1–4.

A subtle NNE-trending gravity low of 3 to −5 mGal in the northern Måløy Slope may represent locally deep-lying basement, although this inference is not supported by seismic data interpretation (Fig. 7), magnetic data, and onshore-offshore correlations. Instead, a strong, laterally extensive positive magnetic anomaly (anomaly A5; maximum 285 nT; Figs. 6A and 6B), covering approximately the same area, indicates the presence of either a basement structural high, similar to anomaly A2, or an intrusive body. The locations of ENE-trending, WGR-cored antiforms and synforms documented for the onshore part of the study area (Osmundsen and Andersen, 2001; Figs. 6A and 6B) support our interpretation that large-scale positive magnetic anomalies (i.e., anomaly A2) that have a similar trend and that are located along strike of the onshore structures are likely to be attributed to WGR-cored antiforms. Furthermore, biotite augen gneiss drilled in well 36/1–1 appears to confirm the presence of a WGR structural high in the northernmost part of the Måløy Slope.

STRUCTURAL ARCHITECTURE OF CRYSTALLINE BASEMENT ALONG THE MÅLØY SLOPE

Based on: (1) the spatial distributions of SF1–SF4 and SFRa–SFRc, and (2) the lithological and geometrical constraints derived from analysis of well-log, core, and gravity and magnetic anomaly maps, we mapped the four principal basement units (i.e., WGR, NSDZ, allochthons, and Devonian sediments) in three dimensions along the Måløy Slope. The interpreted gross structural architecture of the crystalline basement is illustrated on a N-S–trending seismic profile that connects the offshore with the onshore geology (Fig. 7; a large-scale version of Fig. 7 is presented in Data Repository Item DR5). Characteristic, moderately continuous, high-amplitude reflections of SF3 are clearest, separating discontinuous reflections of SF2 and SF4 (i.e., SFRb; Figs. 4B and 4D). Mylonitic rocks (i.e., SF3; Fig. 4C) form a 2–4-km-thick, highly reflective band that is folded into large-scale (maximum amplitude: ~8 km, wavelength: ~50 km), gently W-plunging, E-trending antiforms and synforms (Fig. 7). This thick mylonitic band is suspected to represent the offshore continuation of a major onshore shear zone, the NSDZ, which deforms rocks of the WGR and allochthons. Average dip angles of the shear zone mapped offshore are in agreement with published estimates from onshore studies (Norton, 1987; Labrousse et al., 2002; Johnston et al., 2007; Vetti, 2008; Templeton, 2015), varying between 10° and 17° on E-trending sections, and reaching up to 35° on the flanks of antiforms (Fig. 7C). The top of the WGR is approximated by the base of the NSDZ and locally by the top basement reflection (Fig. 7). The overall geometry of the WGR is thus characterized by two, gently W-dipping, antiforms in the northern and southern Måløy Slope, with these structures connected by an ~35-km-wide synform resembling the large, folded basement structure inferred from gravity and magnetic anomaly maps (Fig. 6). Furthermore, boreholes 36/1–1 and 36/7–1 provide evidence that rocks attributed to the WGR indeed sub-crop top basement in areas where WGR-cored antiforms are expected to be present.

Consequently, the up to 5-km-thick portion of the basement contained within gently W-plunging synforms of the WGR and NSDZ likely consists of allochthonous material and possibly Devonian sediments (Fig. 1B). The dominant intrabasement reflection types in the central part of the study area are classified as SF2, which we interpret to represent allochthonous material. Lithologies typical for the Lower and Middle Allochthon are reported from six boreholes (Table 1), confirming the presence of allochthonous material at top basement level. Furthermore, we observed small- and large-scale internal folding and complex geometrical relationships between individual reflections and reflection packets, which likely indicate a high degree of structural complexity. These findings are consistent with onshore observations from exposed allochthonous units, reflecting the complex, protracted deformation history of the area (e.g., Andersen and Jamtveit, 1990; Andersen et al., 1994; Osmundsen and Andersen, 2001; Johnston et al., 2007).

The uppermost part of the crystalline basement locally comprises reflections of SF1, which may reflect either allochthons or metasediments of the Devonian basins. The ~2-km-thick unit of subparallel, almost stratified reflections locally appears to unconformably overlie reflections of SF2 (Fig. 7), suggesting the presence of a depositional, albeit unconformable, contact between Devonian sediments and the allochthon. However, because none of the basement-penetrating boreholes on the Måløy Slope encountered Devonian sediments, an alternative source of the observed subparallel reflectivity must be considered (see below).

2-D FORWARD MODELING OF GRAVITY AND MAGNETIC DATA

The largest uncertainties associated with our interpretation of the seismic reflection and gridded gravity and magnetic anomaly data are associated with: (1) the presence or absence of Devonian metasediments offshore west Norway; and (2) whether changes in seismic facies and reflection patterns effectively represent different lithological units with particular density and magnetic properties. We therefore used 2-D forward modeling of gravity and magnetic data to mitigate these uncertainties, choosing a simple approach that drew on our observations of the basement geology onshore and offshore western Norway. Step-by-step details about the modeling procedure and the associated uncertainties are provided in Data Repository Items DR3 and DR4.

Figure 8 shows the final density and magnetic forward model we generated along the same N-trending seismic profile as shown in Figure 7. Our interpretation supports the presence of a WGR-cored antiform in the southern and northern Måløy Slope (Fig. 8). Note that the model requires the presence of a northern, WGR-cored structural high, although it is not clearly reflected in the amplitude of the gravity signal or in the gridded Bouguer gravity anomaly map (anomaly A5 in Fig. 6A). The absence of a strong gravity anomaly is explained by the similar density values of adjacent basement blocks in the area, which do not cause lateral density contrasts large enough to create a pronounced anomaly. Furthermore, the required lower-density values for the WGR in the north compared to the south are in agreement with an overall northward decrease in average rock densities within the WGR onshore (cf. Olesen et al., 2010).

To explain the high-amplitude, long-wavelength magnetic anomaly in the north (Fig. 8), we had to introduce two highly magnetic blocks to the model at deeper basement levels. We infer that the smaller of these two blocks represents an intrusive body forming part of the series of at least four positive magnetic anomalies that are observed further north along the Norwegian coastline (Olesen et al., 2010). This interpretation is supported by boreholes 6306/10–1 and 6305/12–2, which are located above one of those magnetic anomalies, and which encountered intrusive, granitic rocks within basement (for details, see Data Repository Item DR6). However, we could not observe a distinct seismic facies (e.g., high-amplitude, crosscutting or discordant seismic facies) that could be readily attributed to an intrusive igneous body. The lack of reflectivity may be explained by minimal density and P-wave velocity contrasts and therefore reflection coefficients that may be too small to generate reflections distinguishable from noise. Moreover, gradational or irregular contacts between the intrusion and the country rock, or a largely homogeneous intrusion, may cause poor imaging of the postulated intrusion (Johnson, 1990; Smithson and Johnson, 2003). We interpret the second highly magnetic block (2.8 g/cm^3/0.013 SI) to reflect a part of the WGR that is more strongly magnetized than its surroundings, and that may therefore comprise a more mafic portion of the WGR.

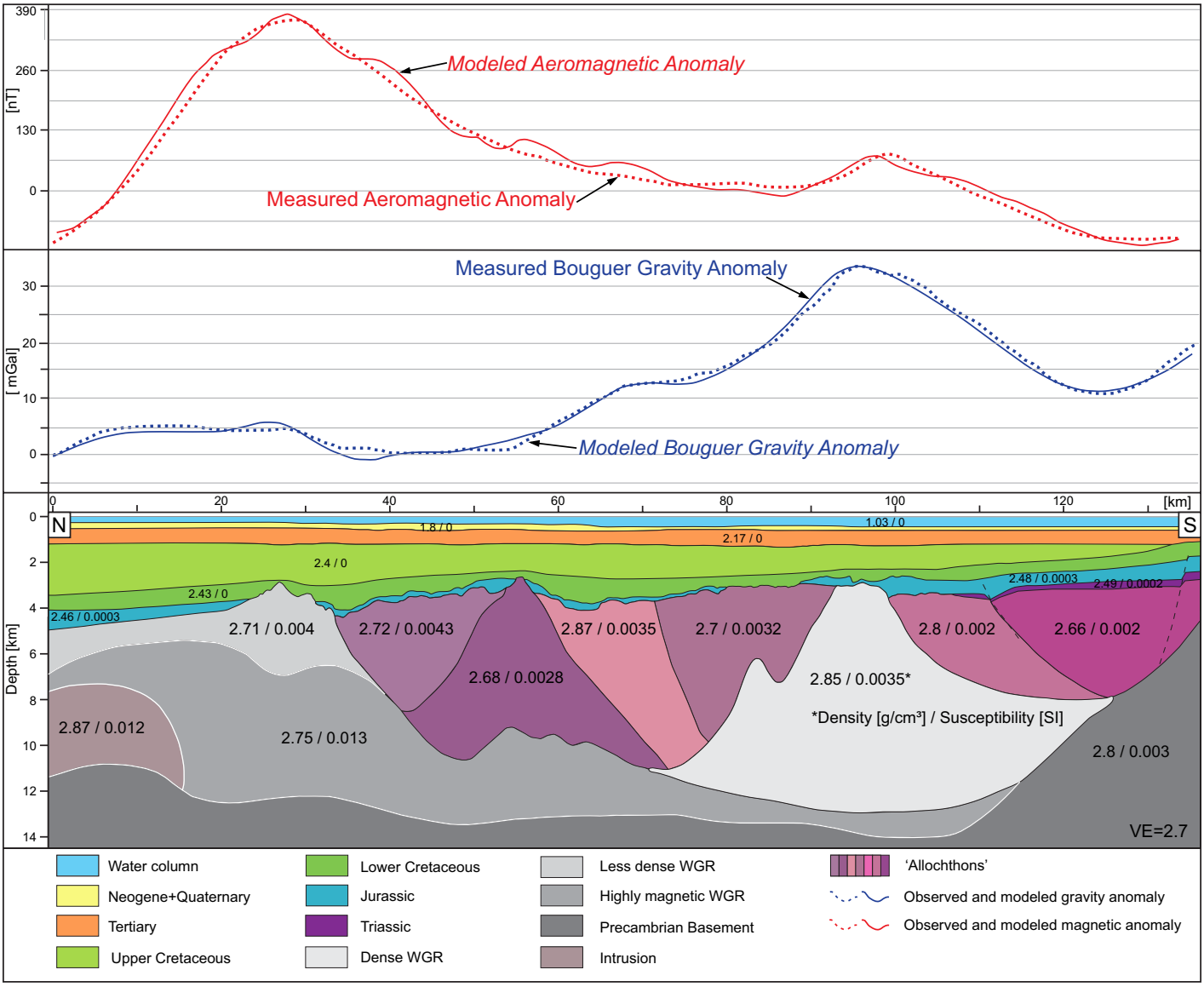

Figure 8. Gravity and magnetic forward modeling carried out along the seismic transect shown in Figure 6. Dotted anomaly curves represent the measured data, whereas solid lines represent the modeled anomalies. Boundaries of basement bodies constrained by seismic data are shown in black and were kept fixed during the modeling. White lines show the outlines of basement bodies that needed to be introduced to the model to achieve a better fit between measured and modeled aeromagnetic anomaly curves. Top of the lower crust and mantle are not shown but were set to a constant depth of 23 km (Olesen et al., 2010) and 30 km (Ebbing et al., 2012; Maupin et al., 2013), respectively. VE—vertical exaggeration; WGR—Western Gneiss Region.

The high degree of lithological heterogeneity within the allochthons suggests that the density distribution within this unit is more complex than in the WGR (Table 2). To capture this heterogeneity in our 2-D model, we assumed that the juxtaposition of different allochthonous rock types is reflected in the observed large-scale changes in the character and geometry of seismic reflection patterns within the interpreted allochthons. We therefore used boundaries between different reflection patterns to divide the allochthons into several blocks, as indicated by the yellow dashed lines in Figure 7C. Despite introducing more uncertainty to the model with this procedure, dividing the allochthons into several blocks with distinct density and susceptibility allowed us to generate a better fit between the observed and modeled gravity and magnetic anomalies (Data Repository Item DR3).

A comparatively dense block (2.87 g/cm^3) in the central part of the profile correlates with the ~10-km-wide zone of steep S- to SW-dipping reflections of SFRc (Fig. 5C), which we interpret as a zone of intense deformation. If our interpretation is correct, the increased density value may reflect high-density rock types such as anorthosites, amphibolites, gabbros, and/or greenschist within a shear zone (Table 2; see NGU onshore petrophysical database, http://aps.ngu.no/kart/geofysikk/). These rock types are observed within the strongly mylonitized NSDZ in the area of Florø and Eikefjord onshore (Fig. 1A; Bryhni and Lutro, 2000a, 2000b; Lutro and Bryhni, 2000). Alternatively, greenschists or gabbros associated with ophiolites of the Upper Allochthon could explain the elevated density, but not the low magnetic susceptibility of the block. Unfortunately, the model could not be used to either confirm or disprove

the presence of Devonian sediments on the Måløy Slope, as average density and magnetic properties of Devonian sediments and allochthons appear too similar to have a noticeable effect on the observed gravity and magnetic anomalies (Table 2).

Despite the ambiguity inherent in the interpretation of potential field data, the model we present here provides one geologically plausible solution that is broadly consistent with the seismic facies variability observed within reflection data, and the geometry of basement structures confidently mapped just onshore. Uncertainties remain with respect to the range of density and susceptibility values that can occur within each rock type (Table 2), the exact depth and geometry of source bodies, and the effects of potential lower-crustal heterogeneity.

DISCUSSION

Link Between Intrabasement Seismic Reflectivity and Basement Structural Architecture and Composition

We have shown that different basement units (WGR, allochthons, and NSDZ) can be distinguished by their seismic characteristics and physical properties (Table 2; Fig. 8). We here discuss briefly the factors that may contribute to these different seismic characters.

SF1

The simplest explanation for subparallel reflections is compositional layering, which could be caused by tens-to-hundred-meter-thick coarsening-upward cycles within Devonian metasediments, comparable to those observed onshore (Steel, 1976; Steel et al., 1977; Steel and Aasheim, 1977). However, borehole data, and gravity and magnetic forward modeling do not confirm the presence of Devonian metasediments on the Måløy Slope. Alternatively, compositional layering may occur within the allochthons. Onshore geological data show that the allochthons are composed of a variety of accreted terranes and stacked felsic and mafic rock types of varying metamorphic grade (e.g., Andersen et al., 1994; Gee et al., 2008; Hacker et al., 2010); as a result, compositional layering can at least partly explain the observed basement reflectivity.

Since SF1 is exclusively observed in the uppermost part of the crystalline basement (up to 2 km below top acoustic basement), we also consider different degrees of weathering and fluid-filled fracture networks as potential causes for subparallel reflection patterns. Our borehole analysis confirmed that the uppermost part of the crystalline basement is likely weathered and/or contains fluid-filled fractures. The presence of fluids can decrease the P-wave velocity of a rock unit by up to 20% (e.g., Goodwin and Thompson, 1988; Johnson and Hartman, 1991; Smithson et al., 2000; Healy et al., 2009), which can lead to strong impedance contrasts, and therefore, high-amplitude reflections that may be stronger than reflections from primary lithological changes (Hyndman and Shearer, 1989; Harjes et al., 1997). Fluid-filled fractures can cause scattering and crosscutting horizontal reflections (Ganchin et al., 1998). Fractures and joints of all scales and varying orientations are furthermore a common feature of the rocks exposed onshore (Fossen et al., 2016). These observations suggest that fluid-filled fractures may play a major role in the reflectivity of the upper parts of the crystalline basement, provided that such fracture systems have a strong horizontal component and thus are imaged by seismic reflection data.

SF2

We interpret the allochthonous basement units to be characterized by often folded, medium- to high-amplitude, laterally discontinuous reflections within otherwise acoustically transparent or chaotic seismic facies (SF2, Fig. 4). Folded reflections are assumed to represent either large-scale migmatitic structures (Mehnert, 1968) or folded layers of different lithologies (Figs. 4B and 7). In response to the extensive Devonian deformation, gneisses are expected to have formed migmatites within the basement, a common metamorphic rock type characterized by alternating millimeter- to kilometer-thick, felsic and mafic layers; such pronounced lithological heterogeneity may cause prominent intracrystalline basement reflections (e.g., Kern et al., 2002; Smithson and Johnson, 2003). Based on onshore observations (e.g., Bryhni and Lutro, 2000a, 2000b; Andersen et al., 1994; Osmundsen and Andersen, 2001; Johnston et al., 2007), subseismic, upright and recumbent isoclinal folds are expected to further contribute to the seismic wave field, forming scatterers or packages of discontinuous reflections, respectively (Smithson and Johnson, 2003).

SF3

High-amplitude, relatively continuous reflections and reflection packets of SF3 are interpreted as mylonitic shear bands; these formed within the NSDZ during Devonian extension (Fig. 4C). Shear zones often form pronounced continuous reflections and reflection packets due to their planar geometry and layering, and high densities and P-wave velocities. However, shear zones can locally also have the characteristics of a diffractor because of their complex internal architecture (folding, lensing, boudinage; e.g., Smythe et al., 1982; Fountain et al., 1984; Hurich et al., 1985; Christensen and Szymanski, 1988; Wang et al., 1989; Kern and Wenk, 1990; McDonough and Fountain, 1988; de Wit et al., 2001). Therefore, abrupt terminations of high-amplitude reflections within SF3 are likely to be caused by lateral changes in composition, strain, orientation to the seismic wave front (Brocher and Christensen, 1990; McDonough and Fountain, 1988), and/or structural complexity of the mylonitic rock body itself. The mineralogical composition of the shear zone remains speculative, but it is likely to consist of several, strongly sheared rock types. Onshore west Norway, different rock types within the NSDZ are classified as "mylonites," with compositions ranging from quartzites to mica schists, anorthosites, amphibolites, greenschists, and gneisses (Bryhni and Lutro, 2000a, 2000b; Lutro and Bryhni, 2000). These rock types are also likely to be present within the NSDZ offshore, adding to the complexity of the observed seismic reflectivity.

SF4

Reflections classified as SF4, which we infer belong to WGR material, are most clearly observed at depths >12 km (Figs. 4D and 7). The commonly short, apparently crosscutting reflections are suspected to represent large-scale conjugate or doubly vergent S-C fabrics similar to reflection patterns described from mid- and lower-crustal seismic reflection sections elsewhere (Reston, 1988; Varsek and Cook, 1994; Torvela et al., 2013). Furthermore, field studies show that such deformation fabrics exhibit a remarkable self-similarity at a wide range of scales (10^{-8} to 10^{5} m; Hippertt, 1999; Waters et al., 2003), making their seismic imaging plausible. Conjugate S-C fabrics form under coaxial deformation during the late stages of shear zone evolution (Fossen, 2010) and are commonly associated with mylonitic rocks. Therefore, reflections of SF4 can most likely be attributed to the internal mineral and velocity anisotropy and structural complexity of sheared rocks, rather than lithological variations within the WGR. Angles between S and C planes in SF4 vary between 20° and 40°, which are within the range of typically observed values for such fabrics (Fossen, 2010). Another explanation for the reflection geometry observed for SF4 is anastomosing shear zones characterized by individual bands that exhibit different directions of motion. Both conjugate and anastomosing shear zones are defined by higher-strain zones that encase lower-strain (protolithic) lenses (e.g., Hudleston, 1999); these two types of shear zones may become indistinguishable from one another at very high strains as shear bands rotate into parallelism with the shear direction.

Both interpretations indicate that the upper part of the WGR is mylonitic, an interpretation that is consistent with onshore observations. Based on data from the Kvamshesten area, Andersen and Jamtveit (1990) reported a transition in deformation fabrics within the WGR from penetrative simple shear fabrics close to the NSDZ to inhomogeneous pure shear fabrics that are truncated by anastomosing zones of simple shear 2–6 km below the NSDZ. This transition in deformation fabrics, and decrease in strain intensity with depth, can be correlated with the transition from SF3 (high-strain zone; planar mylonitic rocks) to SF4 (medium-strain zone; anastomosing mylonitic shear bands/S-C fabrics). Hence, we conclude that variations of the intrabasement facies and reflection patterns are not only a result of lithological changes, interference, and scattering effects, but they can also be linked to the style and amount of ductile deformation that took place in this and likely other areas (e.g., Klemperer, 1987).

Onshore-Offshore Correlation of Crystalline Basement Units

Through 3-D mapping of the four, laterally correlatable seismic facies (Fig. 4) and three key seismic facies relationships (Fig. 5), and by integrating our seismic interpretation with the onshore geology, borehole data, and 2-D forward modeling of gravity and magnetic data, we constructed a 3-D geometric model of the basement architecture offshore west Norway, relating it to the onshore geology presented by Osmundsen and Andersen (2011; Fig. 9). The geometry of the NSDZ is represented by the physiography of the WGR (Fig. 9C), which correlates to WGR antiforms and synforms onshore (Fig. 9A). WGR synforms only comprise allochthonous basement rocks, since we were unable to find convincing evidence for the presence of Devonian metasediments offshore. The absence of Devonian metasediments on the Måløy Slope suggests either nondeposition or erosion of the sediments during Devonian extension and exhumation. We favor the latter explanation, since very thick (6–7 km) Devonian metasediments are identified within large half grabens further west, on the East Shetland Platform (Platt, 1995; Platt and Cartwright, 1998; Marshall and Hewett, 2003), and in the Orcadian and West Orkney Basins (Norton et al., 1987; Coward, 1990: Wilson et al., 2010), suggesting Devonian sediments were present over a much larger area in the past.

Figure 10 shows a 1:1 scale, E-W cross section illustrating the geometric relationships among the WGR, NSDZ, and Caledonian allochthons on the Måløy Slope as interpreted from seismic data, in comparison to the onshore geology near the Devonian Hornelen Basin. The onshore part of the cross section was derived from literature and geological maps (based on Norton, 1986, 1987; Bryhni and Lutro, 2000a, 2000b; Lutro and Bryhni, 2000; Fossen et al., 2016), although the exact structural configuration below the Hornelen detachment is uncertain (indicated by question marks in Fig. 10). The Hornelen detachment defines the contact between the Hornelen Basin and the underlying mylonitic NSDZ (Fossen et al., 2016). Both the lower part of the allochthons and the upper part of the WGR are incorporated in the NSDZ (Fig. 10). Pink color gradients illustrate the upward and downward decreases in strain in the allochthons and WGR away from the core of the NSDZ, respectively. Geological maps (e.g., Fig. 1A) and published onshore profiles (e.g., Fig. 1B) indicate the presence of the Lower and Middle Allochthons within the NSDZ south, east, and below the Hornelen Basin. The exact thickness of the allochthonous units onshore remains unknown (maximum 5 km; Osmundsen and Andersen, 2001).

Offshore, we interpret a slightly steeper dipping NSDZ, represented by an ~2–4-km-thick, highly reflective (SF3) mylonitic band, separating allochthonous rocks above from the WGR below (Figs. 2 and 10). Here, the allochthons are up to 5 km thick within WGR synforms. The ~23-km-wide coastal area between the Måløy Slope and Hornelen Basin (labeled "Based on magnetic data" in Fig. 10) likely has allochthonous material in the upper part of the crystalline basement (Lutro and Bryhni, 2000). Using gravity and magnetic data, Smethurst (2000) interpreted this area as "Caledonian ophiolite" (= Upper Allochthon, density: 2.85–2.95 g/cm^3; susceptibility: 0.0003–0.001; Olesen et al., 2010). Rocks associated with the Upper Allochthon (greenschists and amphibolites) have a depositional contact with the Devonian Hornelen Basin (Lutro and Bryhni, 2000; Fossen et al., 2016), with Upper Allochthon rocks also present in the nearby Eikefjord and Bremangerlandet areas (Fig. 1A). It therefore seems plausible that crystalline basement along the coastal area offshore Hornelen consists of ophiolitic rocks of the Upper Allochthon.

Our interpretation of the depth and architecture of the WGR and NSDZ shown in Figure 10 has important implications for the location of the suture zone between Baltica and Laurentia. Due to a W-NW–directed increase in metamorphic grade of the WGR onshore, several authors have suggested that the suture zone between Baltica and Laurentia is located beneath the northern North Sea, and that it may have a similar, broadly northerly trend as the North Viking and Sogn grabens (e.g., Fossen, 2000; Lyngsie and Thybo, 2007; Fossen et al., 2016). For similar reasons, Cocks et al. (2005) interpreted the suture zone to follow a NNE-NE trend in the Norwegian Sea. Based on our mapping and interpretation of seismic facies, the NSDZ and WGR (i.e., the eastern edge of Baltica) appear to continue into the Sogn graben (Fig. 10). Considering that reconstructed Caledonian paleopressures from the eastern margin of the Hornelen Basin and Nordfjord area are already very high (20–25 kbar = 65–90 km depth; Wain, 1997; Krabbendam and Dewey, 1998), and assuming a constant dip of the NSDZ of 15°, the WGR must have been subducted to extreme depths of 105–130 km underneath the present-day Sogn graben, ~150 km further east of the Hornelen Basin. However, due to the likelihood of a varying dip angle of the NSDZ and a poor understanding of the post-kinematic rotation history of the NSDZ (Norton, 1986, 1987; Hacker, 2003), these paleodepth values are likely overestimated. Alternatively, the high-amplitude reflections of SF3 that reach the Sogn graben (Figs. 2 and 10) may not belong to the NSDZ, but to a different, so-far-unidentified Devonian shear zone (cf. Fazlikhani et al., 2017).

CONCLUSIONS

Using conventional 2-D and 3-D seismic reflection, borehole, core, and petrophysical data, and 2-D gravity and magnetic forward modeling, as well as onshore-offshore correlations, this study resolved the 3-D geometry and composition of crystalline basement structures offshore west Norway. We have shown the following:

(1) The crystalline basement along the Måløy Slope is characterized by a pronounced compositional and structural heterogeneity. Offshore well-log and core data indicate the presence of different kinds of gneisses that are distinguished by their mineralogy and internal deformation fabrics.

(2) The basement is characterized by a high degree of intrabasement reflectivity that can be divided into four distinct, laterally correlatable seismic facies. Based on our onshore-offshore correlations and well-log and seismic analysis, we suggest that compositional layering and scattering effects caused by subseismic heterogeneity are likely the main causes for the observed intrabasement reflectivity. Furthermore, mylonitic shear zones, zones of intense fracturing, and the limbs of isoclinal and recumbent folds are considered to cause significant reflectivity.

(3) The results of seismic data interpretation show that the basement reflectivity is created by the superimposition of the main basement units in the area, i.e., WGR, NSDZ, Caledonian allochthons, and possibly Devonian sediments. Each unit is distinguished by its seismic character, physical properties, 3-D geometry, stratigraphic position, and spatial relationship to other units.

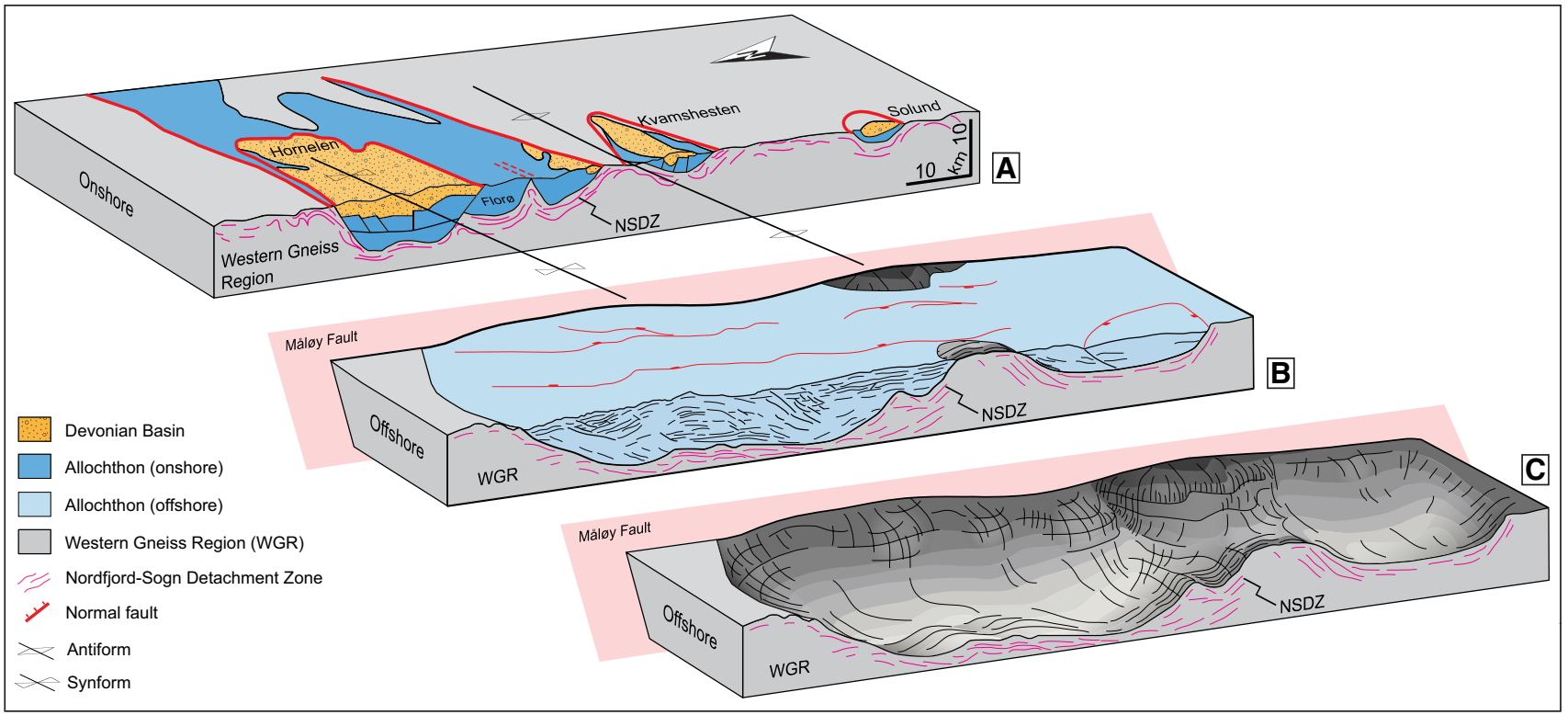

Figure 9. Schematic block diagram illustrating the interpreted offshore crystalline basement architecture in relation to the onshore geology. Geology of onshore block is based on Andersen and Jamtveit (1990) and Osmundsen and Andersen (2001). For completeness, major rift-related normal faults (e.g., Færseth, 1996; Brekke, 2000) are included to illustrate that the basement is truncated and offset by these faults. Note the presence of the W-dipping, normal Måløy fault, which is located along the shelf edge and displaces the crystalline basement by up to 1 km (Bell et al., 2014). NSDZ—Nordfjord-Sogn detachment zone; WGR—Western Gneiss Region.

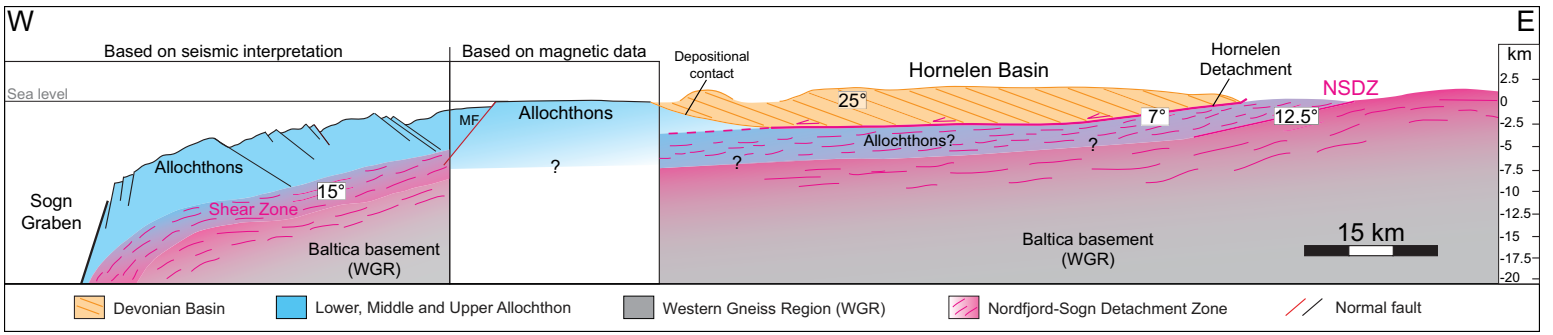

Figure 10. Scaled (1:1) E-W–oriented cross section correlating the interpreted onshore and offshore structural architecture of crystalline basement units in west Norway. The onshore part is based on Norton (1986, 1987), Bryhni and Lutro (2000a, 2000b), Lutro and Bryhni (2000), and Fossen et al. (2016), whereas the offshore part is based on results from this study. Approximate profile location is indicated by the eastward continuation of the seismic profile shown in Figure 2 (see Fig. 1A). MF—Måløy fault; NSDZ—Nordfjord-Sogn detachment zone; WGR—Western Gneiss Region.

(4) Gridded gravity and magnetic data helped us to constrain the location and geometry of large-scale intrabasement synforms and antiforms, to ascertain lateral changes in the physical properties of the basement, and to bridge the gap between offshore 3-D seismic data and the onshore geology.

(5) The interpreted large-scale structural architecture of the crystalline basement offshore west Norway correlates well with onshore structural models (e.g., Osmundsen and Andersen, 2001) and is further constrained by 2-D gravity and magnetic forward modeling. In contrast to previous studies, use of the seismic interpretation of basement structures as geometric constraints for the 2-D gravity and magnetic model is found to be a more robust approach for modeling the distribution of density and magnetic properties in the subsurface.

(6) The basement rock types and structures described in this study are common within deformed continental crust and may thus occur elsewhere. Hence, we consider that the approach employed here can be used in other subsurface studies and that our results are a valuable input for analogue and numerical modeling studies to more realistically model processes such as rift development above heterogeneous substrate.

ACKNOWLEDGMENTS

We would like to thank Equinor ASA for allowing us to show the seismic and borehole data used in this study, along with Schlumberger, Geosoft, and Senergy for providing academic licenses for use of Petrel, Oasis montaj, and Interactive Petrophysics software, respectively. In addition, we would like to thank the Norwegian Geological Survey for the permission to show the gravity and magnetic data. We thank the editor, Tony Doré, and two anonymous reviewers for their thorough and thought-provoking reviews, which substantially improved our initial submission. This study forms part of the MultiRift Project, funded by the Research Council of Norway's PETROMAKS program (project number 215591), and Equinor ASA to the University of Bergen and partners Imperial College, University of Manchester, and University of Oslo.

REFERENCES CITED

Abramovitz, T., and Thybo, H., 2000, Seismic images of Caledonian, lithosphere-scale collision structures in the southeastern North Sea along Mona Lisa Profile 2: Tectonophysics, v. 317, p. 27–54, https://doi.org/10.1016/S0040-1951(99)00266-8.

Ahmadi, O., Koyi, H., Juhlin, C., and Gessner, K., 2016, Seismic signatures of complex geological structures in the Cue-Weld Range area, Murchison domain, Yilgarn craton, Western Australia: Tectonophysics, v. 689, p. 56–66.

Allmendinger, R.W., Nelson, K.D., Potter, C.J., Barazangi, M., Brown, L.D., and Oliver, J.E., 1987, Deep seismic reflection characteristics of the continental crust: Geology, v. 15, p. 304–310, https://doi.org/10.1130/0091-7613(1987)15<304:DSRCOT>2.0.CO;2.

Andersen, T.B., 1998, Extensional tectonics in the Caledonides of southern Norway, an overview: Tectonophysics, v. 285, p. 333–351, https://doi.org/10.1016/S0040-1951(97)00277-1.

Andersen, T.B., and Andresen, A., 1994, Stratigraphy, tectonostratigraphy and the accretion of outboard terranes in the Caledonides of Sunnhordland, W. Norway: Tectonophysics, v. 231, p. 71–84, https://doi.org/10.1016/0040-1951(94)90122-8.

Andersen, T.B., and Jamtveit, B., 1990, Uplift of deep crust during orogenic extensional collapse: A model based on field studies in the Sogn-Sunnfjord region of western Norway: Tectonics, v. 9, no. 5, p. 1097–1111, https://doi.org/10.1029/TC009i005p01097.

Andersen, T.B., Jamtveit, J., Dewey, J.F., and Swensson, E., 1991, Subduction and eduction of continental crust: Major mechanisms during continent-continent collision and orogenic extensional collapse, a model based on the south Norwegian Caledonides: Terra Nova, v. 3, no. 3, p. 303–310, https://doi.org/10.1111/j.1365-3121.1991.tb00148.x.

Andersen, T.B., Osmundsen, P.T., and Jolivet, L., 1994, Deep crustal fabrics and a model for the extensional collapse of the southwest Norwegian Caledonides: Journal of Structural Geology, v. 16, no. 9, p. 1191–1203, https://doi.org/10.1016/0191-8141(94)90063-9.

Andresen, A., Rehnström, E.F., and Holte, M., 2007, Evidence for simultaneous contraction and extension at different crustal levels during the Caledonian orogeny in NE Greenland: Journal of the Geological Society, [London] v. 164, no. 4, p. 869–880, https://doi.org/10.1144/0016-76492005-056.

Bartetzko, A., Delius, H., and Pechnig, R., 2005, Effect of compositional and structural variations on log responses of igneous and metamorphic rocks. I: Mafic rocks, *in* Harvey, P.K., Brewer, T.S., Pezard, P.A., and Petroc, V.A., eds., Petrophysical Properties of Crystalline Rocks: Geological Society, London, Special Publication 240, p. 255–278, https://doi.org/10.1144/GSL.SP.2005.240.01.19.

Bartholomew, I.D., Peters, J.M., and Powell, C.M., 1993, Regional structural evolution of the North Sea: Oblique slip and the reactivation of basement lineaments: Geological Society, London, Petroleum Geology Conference Series, v. 4, p. 1109–1122.

Bell, R.E., Jackson, C.A.L., Whipp, P.S., and Clements, B., 2014, Strain migration during multiphase extension: Observations from the northern North Sea: Tectonics, v. 33, no. 10, p. 1936–1963, https://doi.org/10.1002/2014TC003551.

Bingen, B., Nordgulen, O., and Viola, G., 2008, A four-phase model for the Sveconorwegian orogeny, SW Scandinavia: Norsk Geologisk Tidsskrift, v. 88, p. 43–72.

Bird, P.C., Cartwright, J.A., and Davies, T.L., 2015, Basement reactivation in the development of rift basins: An example of reactivated Caledonide structures in the West Orkney Basin: Journal of the Geological Society [London], v. 172, no. 1, p. 77–85, https://doi.org/10.1144/jgs2013-098.

Bongajum, E., Milkereit, B., Adam, E., and Meng, Y., 2012, Seismic imaging in hardrock environments: The role of heterogeneity?: Tectonophysics, v. 572, p. 7–15, https://doi.org/10.1016/j.tecto.2012.03.003.

Brekke, H., 2000, The tectonic evolution of the Norwegian Sea continental margin, with emphasis on the Vøring and Møre basins: Geological Society, London, Special Publications, v. 167, p. 327–378.

Brewer, J.A., and Smythe, D.K., 1984, MOIST and the continuity of crustal reflector geometry along the Caledonian-Appalachian orogen: Journal of the Geological Society [London], v. 141, no. 1, p. 105–120, https://doi.org/10.1144/gsjgs.141.1.0105.

Brocher, T.M., and Christensen, N.I., 1990, Seismic anisotropy due to preferred mineral orientation observed in shallow crustal rocks in southern Alaska: Geology, v. 18, no. 8, p. 737–740, https://doi.org/10.1130/0091-7613(1990)018<0737:SADTPM>2.3.CO;2.

Bryhni, I., and Lutro, O., 2000a, Naustdal Berggrundnsgeologisk Kart 1218II: Trondheim, Norges Geologiske Undersøkelse, scale 1:50,000.

Bryhni, I., and Lutro, O., 2000b, Berggrunnskart Eikefjord 1118II: Trondheim, Norges Geologiske Undersøkelse, scale 1:50,000.

Chauvet, A., and Séranne, M., 1994, Extension-parallel folding in the Scandinavian Caledonides: Implications for late-orogenic processes: Tectonophysics, v. 238, p. 31–54, https://doi.org/10.1016/0040-1951(94)90048-5.

Cheadle, M.J., McGeary, S., Warner, M.R., and Matthews, D.H., 1987, Extensional structures on the western UK continental shelf: A review of evidence from deep seismic profiling, *in* Coward, M.P., Dewey, J.F., and Hancock, P.L., eds., Continental Extensional Tectonics: Geological Society, London, Special Publication 28, p. 445–465, https://doi.org/10.1144/GSL.SP.1987.028.01.28.

Christensen, N.I., and Szymanski, D.L., 1988, Origin of reflections from the Brevard fault zone: Journal of Geophysical Research–Solid Earth, v. 93, no. B2, p. 1087–1102, https://doi.org/10.1029/JB093iB02p01087.

Cocks, L., Robin, M., and Trond, H., 2005, Torsvik Baltica from the late Precambrian to mid-Palaeozoic times: The gain and loss of a terrane's identity: Earth-Science Reviews, v. 72, no. 1–2, p. 39–66, https://doi.org/10.1016/j.earscirev.2005.04.001.

Cook, F.A., van der Velden, A.J., and Hall, K.W., 1999, Frozen subduction in Canada's Northwest Territories: Lithoprobe deep lithospheric reflection profiling of the western Canadian Shield: Tectonics, v. 18, no. 1, p. 1–24, https://doi.org/10.1029/1998TC900016.

Coward, M.P., 1990, The Precambrian, Caledonian and Variscan framework to NW Europe, *in* Hardman, R.F.P., and Brooks, J., eds., Tectonic Events Responsible for Britain's Oil and Gas Reserves: Geological Society, London, Special Publication 55, p. 1–34, https://doi.org/10.1144/GSL.SP.1990.055.01.01.

Coward, M.P., Enfield, M.A., and Fischer, M.W., 1989, Devonian basins of northern Scotland: Extension and inversion related to Late Caledonian–Variscan tectonics, *in* Cooper, M.A., and Williams, G.D., eds., Inversion Tectonics: Geological Society, London, Special Publication 44, p. 275–308, https://doi.org/10.1144/GSL.SP.1989.044.01.16.

Cowie, P.A., Gupta, S., and Dawers, N.H., 2000, Implications of fault interaction for early syn-rift sedimentation: Insights from a numerical fault growth model: Basin Research, v. 12, p. 241–261, https://doi.org/10.1046/j.1365-2117.2000.00126.x.

Cuong, T.X., and Warren, J.K., 2009, Bach Ho Field, a fractured granitic basement reservoir, Cuu Long Basin, offshore SE Vietnam: A buried-hill play: Journal of Petroleum Geology, v. 32, no. 2, p. 129–156, https://doi.org/10.1111/j.1747-5457.2009.00440.x.

Cuthbert, S.J., 1991, Evolution of the Devonian Hornelen Basin, west Norway: New constraints from petrological studies of metamorphic clasts, *in* Morton, A.C., Todd, S.P., and Haughton, P.D.W., eds., Developments in Sedimentary Provenance Studies: Geological Society, London, Special Publication 57, p. 343–360, https://doi.org/10.1144/GSL.SP.1991.057.01.25.

Dewey, J.F., and Strachan, R.A., 2003, Changing Silurian–Devonian relative plate motion in the Caledonides: Sinistral transpression to sinistral transtension: Journal of the Geological Society [London], v. 160, no. 2, p. 219–229, https://doi.org/10.1144/0016-764902-085.

Dewey, J.F., Ryan, P.D., and Andersen, T.B., 1993, Orogenic uplift and collapse, crustal thickness, fabrics and metamorphic phase changes: The role of eclogites, *in* Prichard, H.M., Alabaster, T., Harris, N.B.W., and Neary, C.R., eds., Magmatic Processes and Plate Tectonics: Geological Society, London, Special Publication 76, p. 325–343, https://doi.org/10.1144/GSL.SP.1993.076.01.16.

de Wit, M.J., Bowring, S.A., Ashwal, L.D., Randrianasolo, L.G., Morel, V P., and Rambeloson, R.A., 2001, Age and tectonic evolution of Neoproterozoic ductile shear zones in southwestern Madagascar, with implications for Gondwana studies: Tectonics, v. 20, no. 1, p. 1–45, https://doi.org/10.1029/2000TC900026.

Doré, A.G., Lundin, E.R., Fichler, C., and Olesen, O., 1997, Patterns of basement structure and reactivation along the NE Atlantic margin: Journal of the Geological Society [London], v. 154, no. 1, p. 85–92, https://doi.org/10.1144/gsjgs.154.1.0085.

Ebbing, J., Lundin, E., Olesen, O., and Hansen, E.K., 2006, The mid-Norwegian margin: A discussion of crustal lineaments, mafic intrusions, and remnants of the Caledonian root by 3-D density modelling and structural interpretation: Journal of the Geological Society [London], v. 163, no. 1, p. 47–59, https://doi.org/10.1144/0016-764905-029.

Ebbing, J., England, R.W., Korjad, T., Lauritsen, T., Olesen, O., Stratford, W., and Weidle, C., 2012, Structure of the Scandes lithosphere from surface to depth: Tectonophysics, v. 536–537, p. 1–24, https://doi.org/10.1016/j.tecto.2012.02.016.

Eide, E.A., Torsvik, T.H., and Andersen, T.B., 1997, Absolute dating of brittle fault movements: Late Permian and Late Jurassic extensional fault breccias in western Norway: Terra Nova, v. 9, no. 3, p. 135–139, https://doi.org/10.1046/j.1365-3121.1997.d01-21.x.

Eide, E.A., Torsvik, T.H., Andersen, T.B., and Arnaud, N.O., 1999, Early Carboniferous unroofing in western Norway: A tale of alkali feldspar thermochronology: The Journal of Geology, v. 107, no. 3, p. 353–374, https://doi.org/10.1086/314351.

Engvik, A.K., and Andersen, T.B., 2000, Evolution of Caledonian deformation fabrics under eclogite and amphibolite facies at Vardalsneset, Western Gneiss Region, Norway: Journal of Metamorphic Geology, v. 18, no. 3, p. 241–257, https://doi.org/10.1046/j.1525-1314.2000.00252.x.

Færseth, R.B., 1996, Interaction of Permo-Triassic and Jurassic extensional fault-blocks during the development of the northern North Sea: Journal of the Geological Society [London], v. 153, no. 6, p. 931–944, https://doi.org/10.1144/gsjgs.153.6.0931.

Færseth, R.B., Gabrielsen, R.H., and Hurich, C.A., 1995, Influence of basement in structuring of the North Sea basin, offshore southwest Norway: Norsk Geologisk Tidsskrift, v. 75, p. 105–119.

Fazlikhani, H., Fossen, H., Gawthorpe, R., Faleide, J.I., and Bell, R.E., 2017, Basement structure and its influence on the structural configuration of the northern North Sea rift: Tectonics, v. 36, p. 1151–1177, https://doi.org/10.1002/2017TC004514.

Fossen, H., 1992, The role of extensional tectonics in the Caledonides of south Norway: Journal of Structural Geology, v. 14, p. 1033–1046, https://doi.org/10.1016/0191-8141(92)90034-T.

Fossen, H., 2000, Extensional tectonics in the Caledonides: Synorogenic or postorogenic?: Tectonics, v. 19, no. 2, p. 213–224, https://doi.org/10.1029/1999TC900066.

Fossen, H., 2010, Structural Geology: Cambridge, UK, Cambridge University Press, 463 p., https://doi.org/10.1017/CBO9780511777806.

Fossen, H., and Dunlap, J.W., 1998, Timing and kinematics of Caledonian thrusting and extensional collapse, southern Norway: Evidence from $^{40}Ar/^{39}Ar$ thermochronology: Journal of Structural Geology, v. 20, no. 6, p. 765–781, https://doi.org/10.1016/S0191-8141(98)00007-8.

Fossen, H., Teyssier, C., and Whitney, D.L., 2013, Transtensional folding: Journal of Structural Geology, v. 56, p. 89–102, https://doi.org/10.1016/j.jsg.2013.09.004.

Fossen, H., Khani, H.F., Faleide, J.I., Ksienzyk, A.K., and Dunlap, W.J., 2016, Post-Caledonian extension in the west Norway–northern North Sea region: The role of structural inheritance, *in* Childs, C., Holdsworth, R.E., Jackson, C.A.-L., Manzocchi, T., Walsh, J.J., and Yielding, G., eds., The Geometry and Growth of Normal Faults: Geological Society, London, Special Publication 439, p. 465–486.

Fountain, D.M., Hurich, C.A., and Smithson, S.B., 1984, Seismic reflectivity of mylonite zones in the crust: Geology, v. 12, no. 4, p. 195–198, https://doi.org/10.1130/0091-7613(1984)12<195:SROMZI>2.0.CO;2.

Ganchin, Y.V., Smithson, S.B., Morozov, I.B., Smythe, D.K., Garipov, V.Z., Karaev, N.A., and Kristofferson, Y., 1998, Seismic studies around the Kola superdeep borehole, Russia: Tectonophysics, v. 288, p. 1–16, https://doi.org/10.1016/S0040-1951(97)00280-1.

Gawthorpe, R.L., and Leeder, M.R., 2000, Tectono-sedimentary evolution of active extensional basins: Basin Research, v. 12, p. 195–218, https://doi.org/10.1046/j.1365-2117.2000.00121.x.

Gee, D.G., Fossen, H., Henriksen, N., and Higgins, A.K., 2008, From the early Paleozoic platforms of Baltica and Laurentia to the Caledonide orogen of Scandinavia and Greenland: Episodes, v. 31, no. 1, p. 44–51.

Gernigon, L., and Brönner, M., 2012, Late Palaeozoic architecture and evolution of the southwestern Barents Sea: Insights from a new generation of aeromagnetic data: Journal of the Geological Society [London], v. 169, no. 4, p. 449–459, https://doi.org/10.1144/0016-76492011-131.

Gilotti, J.A., and McClelland, W.C., 2008, Geometry, kinematics and timing of extensional faulting in the Greenland Caledonides—A synthesis, *in* Higgins, A.K., Gilotti, J.A., and Smith, M.P., eds., The Greenland Caledonides: Evolution of the Northeast Margin of Laurentia: Geological Society of America Memoir 202, p. 251–271, https://doi.org/10.1130/2008.1202(10).

Goff, J.A., and Holliger, K., eds., 2003, Heterogeneity in the Crust and Upper Mantle; Nature, Scaling and Seismic Properties: New York, Kluwer Academic/Plenum Publishers, 349 p., https://doi.org/10.1007/978-1-4615-0103-9.

Goodwin, E.B., and Thompson, G.A., 1988, The seismically reflective crust beneath highly extended terranes: Evidence for its origin in extension: Geological Society of America Bulletin, v. 100, no. 10, p. 1616–1626, https://doi.org/10.1130/0016-7606(1988)100<1616:TSRCBH>2.3.CO;2.

Gupta, S., Cowie, P.A., Dawers, N.H., and Underhill, J.R., 1998, A mechanism to explain rift-basin subsidence and stratigraphic patterns through fault-array evolution: Geology, v. 26, no. 7, p. 595–598, https://doi.org/10.1130/0091-7613(1998)026<0595:AMTERB>2.3.CO;2.

Hacker, B.R., and Gans, P.B., 2005, Continental collisions and the creation of ultrahigh-pressure terranes: Petrology and thermochronology of nappes in the central Scandinavian Caledonides: Geological Society of America Bulletin, v. 117, p. 117–134, https://doi.org/10.1130/B25549.1.

Hacker, B.R., Andersen, T.B., Root, D.B., Mehl, L., Mattinson, J.M, and Wooden, J.L., 2003, Exhumation of high-pressure rocks beneath the Solund Basin, western gneiss region of Norway: Journal of Metamorphic Geology, v. 21, p. 613–629.

Hacker, B.R., Andersen, T.B., Johnston, S., Kylander-Clark, A.R.C., Peterman, E.M., Walsh, E.O., and Young, D., 2010, High-temperature deformation during continental-margin subduction & exhumation: The ultrahigh-pressure Western Gneiss Region of Norway: Tectonophysics, v. 480, p. 149–171, https://doi.org/10.1016/j.tecto.2009.08.012.

Hansen, J., Skjerlie, K.P., Pedersen, R.B., and De La Rosa, J., 2002, Crustal melting in the lower parts of island arcs: An example from the Bremanger granitoid complex, west Norwegian Caledonides: Contributions to Mineralogy and Petrology, v. 143, no. 3, p. 316–335, https://doi.org/10.1007/s00410-001-0342-5.

Harjes, H.-P, Bram, K., Dürbaum, H.-J., Gebrande, H., Hirschmann, G., Janik, M., Klöckner, M., Lüschen, E., Rabbel, W., Simon, M., Thomas, R., Tormann, J., and Wenzel, F., 1997, Origin and nature of crystal reflections: Results from integrated seismic measurements at the KTB superdeep drilling site: Journal of Geophysical Research–Solid Earth, v. 102, no. B8, p. 18,267–18,288, https://doi.org/10.1029/96JB03801.

Hartz, E.H., Martinsen, B.B., Øverli, P.E., Lie, H., Ditcha, E.M., Schmid, D.W., and Medvedev, S., 2013, Newly discovered giant oil fields of North Sea—The role of fractured basement highs, *in* First European Association of Geoscientists and Engineers (EAGE) and Brazilian Geophysical Society (SBGf) Workshop: Fractures in Conventional and Unconventional Reservoirs, Extended Abstracts: Rio de Janeiro, Brazil, 4 p. https://doi.org/10.3997/2214-4609.20131805.

Healy, D., Reddy, S.M., Timms, N.E., Gray, E.M., and Brovarone, A.V., 2009, Trench-parallel fast axes of seismic anisotropy due to fluid-filled cracks in subducting slabs: Earth and Planetary Science Letters, v. 283, p. 75–86, https://doi.org/10.1016/j.epsl.2009.03.037.

Hedin, P., Juhlin, C., and Gee, D.G., 2012, Seismic imaging of the Scandinavian Caledonides to define ICDP drilling sites: Tectonophysics, v. 554, p. 30–41.

Hedin, P., Malehmir, A., Gee, D.G., Juhlin, C., and Dyrelius, D., 2014, 3-D interpretation by integrating seismic and potential field data in the vicinity of the proposed COSC-1 drill site, central Swedish Caledonides, *in* Corfu, F., Gasser, D., and Chew, D.M., eds., New Perspectives on the Caledonides of Scandinavia and Related Areas: Geological Society, London, Special Publication 390, p. 301–319, https://doi.org/10.1144/SP390.15.

Hedin, P., Almqvist, B., Berthet, T., Juhlin, C., Buske, S., Simon, H., Giese, R., Krauß, F., Rosberg, J.-E., and Alm, P.G., 2016, 3-D reflection seismic imaging at the 2.5 km deep COSC-1 scientific borehole, central Scandinavian Caledonides: Tectonophysics, v. 689, p. 40–55.

Hippertt, J., 1999, 20th Anniversary Special Issue: Questions in structural geology—Are SC structures, duplexes and conjugate shear zones different manifestations of the same scale-invariant phenomenon?: Journal of Structural Geology, v. 21, no. 8, p. 975–984, https://doi.org/10.1016/S0191-8141(99)00047-4.

Hudleston, P., 1999, Strain compatibility and shear zones: Is there a problem?: Journal of Structural Geology, v. 21, no. 8, p. 923–932, https://doi.org/10.1016/S0191-8141(99)00060-7.

Huismans, R.S., and Beaumont, C., 2008, Complex rifted continental margins explained by dynamical models of depth-dependent lithospheric extension: Geology, v. 36, no. 2, p. 163–166, https://doi.org/10.1130/G24231A.1.

Hurich, C.A., Smithson, S.B., Fountain, D.M., and Humphreys, M.C., 1985, Seismic evidence of mylonite reflectivity and deep structure in the Kettle Dome metamorphic core complex, Washington: Geology, v. 13, no. 8, p. 577–580, https://doi.org/10.1130/0091-7613(1985)13<577:SEOMRA>2.0.CO;2.

Hyndman, R.D., and Shearer, P.M., 1989, Water in the lower continental crust: Modelling magnetotelluric and seismic reflection results: Geophysical Journal International, v. 98, no. 2, p. 343–365, https://doi.org/10.1111/j.1365-246X.1989.tb03357.x.

Ji, S., and Salisbury, M.H., 1993, Shear-wave velocities, anisotropy and splitting in high-grade mylonites: Tectonophysics, v. 221, p. 453–473.

Johnson, R.A., 1990, Complex response to a "simple" crustal model: Implications for deep crustal reflection interpretation, *in* Green, A.G., ed., Studies of Laterally Heterogeneous Structures Using Seismic Refraction and Reflection Data: Geological Survey of Canada Paper 89-13, p. 213–217.

Johnson, R.A., and Hartman, K.A., 1991, Upper crustal Poisson's ratios in the Colorado Plateau from multicomponent wide-angle seismic recording, *in* Meissner, R., Brown, L., Dürbaum, H., Franke, W., Fuchs, K., and Seifert, F., eds., Continental Lithosphere: Deep Seismic Reflections: Washington, D.C., American Geophysical Union Geodynamics Monograph 22, p. 323–328, https://doi.org/10.1029/GD022p0323.

Johnston, S., Hacker, B.R., and Ducea, M.N., 2007, Exhumation of ultrahigh-pressure rocks beneath the Hornelen zegment of the Nordfjord-Sogn detachment zone, western Norway: Geological Society of America Bulletin, v. 119, p. 1232–1248, https://doi.org/10.1130/B26172.1.

Jones, T.D., and Nur, A., 1984, The nature of seismic reflections from deep crustal fault zones: Journal of Geophysical Research–Solid Earth, v. 89, no. B5, p. 3153–3171, https://doi.org/10.1029/JB089iB05p03153.

Juhojuntti, N., Juhlin, C., and Dyrelius, D., 2001, Crustal reflectivity underneath the central Scandinavian Caledonides: Tectonophysics, v. 334, p. 191–210, https://doi.org/10.1016/S0040-1951(00)00292-4.

Kennett, B.L.N., Yoshizawa, K., and Furumura, T., 2017, Interactions of multi-scale heterogeneity in the lithosphere: Australia: Tectonophysics, v. 717, p. 193–213, https://doi.org/10.1016/j.tecto.2017.07.009.

Kern, H., and Wenk, H.-R., 1990, Fabric-related velocity anisotropy and shear wave splitting in rocks from the Santa Rosa mylonite zone, California: Journal of Geophysical Research–Solid Earth, v. 95, no. B7, p. 11,213–11,223, https://doi.org/10.1029/JB095iB07p11213.

Kern, H., Jin, Z., Gao, S., Popp, T., and Xu, Z., 2002, Physical properties of ultrahigh-pressure metamorphic rocks from the Sulu terrain, eastern central China: Implications for the seismic structure at the Donghai (CCSD) drilling site: Tectonophysics, v. 354, p. 315–330, https://doi.org/10.1016/S0040-1951(02)00339-6.

Kirkpatrick, J.D., Bezerra, F.H.R., Shipton, Z.K., Do Nascimento, A.F., Pytharouli, S.I., Lunn, R.J., and Soden, A.M., 2013, Scale-dependent influence of pre-existing basement shear zones on rift faulting: A case study from NE Brazil: Journal of the Geological Society [London], v. 170, no. 2, p. 237–247, https://doi.org/10.1144/jgs2012-043.

Klemperer, S.L., 1987, Reflectivity of the crystalline crust: Hypotheses and tests: Geophysical Journal International, v. 89, no. 1, p. 217–222, https://doi.org/10.1111/j.1365-246X.1987.tb04411.x.

Knape, A., 1996, Final Well Report Well 36/7–1. Vol. R-076441: Vækerø, Oslo, Norway, Norsk Hydro, 118 p.

Krabbendam, M., and Dewey, J.F., 1998, Exhumation of UHP rocks by transtension in the Western Gneiss Region, Scandinavian Caledonides, *in* Holdsworth, R.E., Strachan, R.A., and Dewey, J.F., eds., Continental Transpressional and Transtensional Tectonics: Geological Society, London, Special Publication 135, p. 159–81, https://doi.org/10.1144/GSL.SP.1998.135.01.11.

Krabbendam, M., Wain, A., and Andersen, T.B., 2000, Pre-Caledonian granulite and gabbro enclaves in the Western Gneiss Region, Norway: Indications of incomplete transition at high pressure: Geological Magazine, v. 137, p. 235–255, https://doi.org/10.1017/S0016756800004015.

Kvarven, T., Mjelde, R., Hjelstuen, B.O., Faleide, J.I., Thybo, H., Flueh, E.R., and Murai, Y., 2016, Crustal composition of the Møre margin and compilation of a conjugate Atlantic margin transect: Tectonophysics, v. 666, p. 144–157.

Labrousse, L., Jolivet, L., Agard, P., Hébert, R., and Andersen, T.B., 2002, Crustal-scale boudinage and migmatization of gneiss during their exhumation in the UHP province of western Norway: Terra Nova, v. 14, no. 4, p. 263–270, https://doi.org/10.1046/j.1365-3121.2002.00422.x.

Lassen, A., and Thybo, H., 2012, Neoproterozoic and Palaeozoic evolution of SW Scandinavia based on integrated seismic interpretation: Precambrian Research, v. 204, p. 75–104, https://doi.org/10.1016/j.precamres.2012.01.008.

Law, A., and Snyder, D.B., 1997, Reflections from a mylonitized zone in central Sweden: Journal of Geophysical Research: Solid Earth, v. 102, p. 8411–8425.

Lorenz, H., Rosberg, J.-E., Juhlin, C., Bjelm, L., Almqvist, B.S.G., Berthet, T., Conze, R., Gee, D.G., Klonowska, I., Pascal, C., Pedersen, K., Roberts, N.M.W., and Tsang, C.-F., 2015, COSC-1—Drilling of a subduction-related allochthon in the Palaeozoic Caledonide orogen of Scandinavia: Scientific Drilling, v. 19, p. 1–11, https://doi.org/10.5194/sd-19-1-2015.

Lutro, O., and Bryhni, I., 2000, Berggrunnskart Florø 1118III: Trondheim, Norges Geologiske Undersökelse, scale 1:50,000.

Lyngsie, S.B., and Thybo, H., 2007, A new tectonic model for the Laurentia–Avalonia–Baltica sutures in the North Sea: A case study along Mona Lisa Profile 3: Tectonophysics, v. 429, p. 201–227, https://doi.org/10.1016/j.tecto.2006.09.017.

Lyngsie, S.B., Thybo, H., and Lang, R., 2007, Rifting and lower crustal reflectivity: A case study of the intracratonic Dniepr-Donets rift zone, Ukraine: Journal of Geophysical Research–Solid Earth, v. 112, no. B12, B12402, https://doi.org/10.1029/2006JB004795.

Marello, L., Ebbing, J., and Gernigon, L., 2010, Magnetic basement study in the Barents Sea from inversion and forward modelling: Tectonophysics, v. 493, p. 153–171, https://doi.org/10.1016/j.tecto.2010.07.014.

Marshall, J.E.A., and Hewett, A.J., 2003, Devonian, *in* Evans, D., Graham, C., Armour, A., and Bathurst, P., eds., The Millennium Atlas: Petroleum Geology of the Central and Northern North Sea: London, Geological Society, p. 65–81.

Maupin, V., Agostini, A., Artemieva, I., Balling, N., Beekman, F., Ebbing, J., England, R.W., Frassetto, A., Gradmann, S., Jacobsen, B.H., Köhler, A., Kvarven, T., Medhus, A.B., Mjelde, R., Ritter, J., Sokoutis, D., Stratford, W., Thybo, H., Wawerzinek, B., and Weidlea, C., 2013, The deep structure of the Scandes and its relation to tectonic history and present-day topography: Tectonophysics, v. 602, p. 15–37.

Mazur, S., Mikolajczak, M., Krzywiec, P., Malinowski, M., Buffenmyer, V., and Lewandowski, M., 2015, Is the Teisseyre-Tornquist zone an ancient plate boundary of Baltica?: Tectonics, v. 34, no. 12, p. 2465–2477, https://doi.org/10.1002/2015TC003934.

McDonough, D.T., and Fountain, D.M., 1988, Reflection characteristics of a mylonite zone based on compressional wave velocities of rock samples: Geophysical Journal International, v. 93, no. 3, p. 547–558, https://doi.org/10.1111/j.1365-246X.1988.tb03880.x.

McGeary, S., and Warner, M.R., 1985, Seismic profiling the continental lithosphere: Nature, v. 317, no. 6040, p. 795–797, https://doi.org/10.1038/317795a0.

Mehnert, K.R., 1968, Migmatites and the Origin of Granitic Rocks: Amsterdam, Elsevier, 393 p.

Meissner, R., Rabbel, W., and Kern, H., 2006, Seismic lamination and anisotropy of the lower continental crust: Tectonophysics, v. 416, no. 1–4, p. 81–99.

Milnes, A.G., Wennberg, O.P., Skår, Ø., and Koestler, A.G., 1997, Contraction, extension and timing in the south Norwegian Caledonides: The Sognefjord transect, *in* Burg, J.-P., and Ford, M., eds., Orogeny Through Time: Geological Society, London, Special Publication 121, p. 123–148, https://doi.org/10.1144/GSL.SP.1997.121.01.06.

Mjelde, R., Kvarven, T., Faleide, J.I., and Thybo, H., 2016, Lower crustal high-velocity bodies along North Atlantic passive margins, and their link to Caledonian suture zone eclogites and early Cenozoic magmatism: Tectonophysics, v. 670, p. 16–29.

Morley, C.K., 2009, Geometry and evolution of low-angle normal faults (LANF) within a Cenozoic high-angle rift system, Thailand: Implications for sedimentology and the mechanisms of LANF development: Tectonics, v. 28, TC5001, https://doi.org/10.1029/2007TC002202.

Morley, C.D., 2010, Stress re-orientation along zones of weak fabrics in rifts: An explanation for pure extension in 'oblique' rift segments?: Earth and Planetary Science Letters, v. 297, p. 667–673.

Morley, C.K., Haranya, C., Phoosongsee, W., Pongwapee, S., Kornsawan, A., and Wonganan, N., 2004, Activation of rift oblique and rift parallel pre-existing fabrics during extension and their effect on deformation style: Examples from the rifts of Thailand: Journal of Structural Geology, v. 26, no. 10, p. 1803–1829, https://doi.org/10.1016/j.jsg.2004.02.014.

Nelson, R., 2001, Geologic Analysis of Naturally Fractured Reservoirs: Boston, Gulf Professional Publishing (Elsevier), 332 p.

Norton, M.G., 1986, Late Caledonide extension in western Norway: A response to extreme crustal thickening: Tectonics, v. 5, no. 2, p. 195–204, https://doi.org/10.1029/TC005i002p00195.

Norton, M.G., 1987, The Nordfjord-Sogn detachment, W. Norway: Norsk Geologisk Tidsskrift, v. 67, no. 2, p. 93–106.

Norton, M.G., McClay, K.R., and Way, N.A., 1987, Tectonic evolution of Devonian basins in northern Scotland and southern Norway: Norsk Geologisk Tidsskrift, v. 67, p. 323.

Olesen, O., Brönner, M., Ebbing, J., Gellein, J., Gernigon, L., Koziel, J., Lauritsen, T., Myklebust, R., Pascal, C., Sand, M., Solheim, D., and Usov, S., 2010, New aeromagnetic and gravity compilations from Norway and adjacent areas: Methods and applications, *in* Vining, B.A., and Pickering, S.C., eds., Petroleum Geology: From Mature Basins to New Frontiers—Proceedings of the 7th Petroleum Geology Conference: London, Geological Society, p. 559–586.

Olyphant, J.R., Johnson, R.A., and Hughes, A.N., 2017, Evolution of the southern Guinea Plateau: Implications on Guinea-Demerara Plateau formation using insights from seismic, subsidence, and gravity data: Tectonophysics, v. 717, p. 358–371, https://doi.org/10.1016/j.tecto.2017.08.036.

Osmundsen, P.T., and Andersen, T.B., 1994, Caledonian compressional and late-orogenic extensional deformation in the Staveneset area, Sunnfjord, western Norway: Journal of Structural Geology, v. 16, p. 1385–1401, https://doi.org/10.1016/0191-8141(94)90004-3.

Osmundsen, P.T., and Andersen, T.B., 2001, The Middle Devonian basins of western Norway: Sedimentary response to large-scale transtensional tectonics?: Tectonophysics, v. 332, p. 51–68, https://doi.org/10.1016/S0040-1951(00)00249-3.

Osmundsen, P.T., Andersen, T.B., and Markussen, S., 1998, Tectonics and sedimentation in the hangingwall of a major extensional detachment: The Devonian Kvamshesten Basin, western Norway: Basin Research, v. 10, no. 2, p. 213–234, https://doi.org/10.1046/j.1365-2117.1998.00064.x.

Paton, D.A., 2006, Influence of crustal heterogeneity on normal fault dimensions and evolution: Southern South Africa extensional system: Journal of Structural Geology, v. 28, no. 5, p. 868–886, https://doi.org/10.1016/j.jsg.2006.01.006.

Phillips, T.B., Jackson, C.A., Bell, R.E., Duffy, O.B., and Fossen, H., 2016, Reactivation of intrabasement structures during rifting: A case study from offshore southern Norway: Journal of Structural Geology, v. 91, p. 54–73, https://doi.org/10.1016/j.jsg.2016.08.008.

Platt, N.H., 1995, Structure and tectonics of the northern North Sea: New insights from deep penetration regional seismic data, *in* Lambiase, J.J., ed., Hydrocarbon Habitat in Rift Basins: Geological Society, London, Special Publication 80, p. 103–113.

Platt, N.H., and Cartwright, J.A., 1998, Structure of the East Shetland Platform, northern North Sea: Petroleum Geoscience, v. 4, no. 4, p. 353–362, https://doi.org/10.1144/petgeo.4.4.353.

Reeve, M.T., Bell, R.E., and Jackson, C.A.-L., 2014, Origin and significance of intra-basement seismic reflections offshore western Norway: Journal of the Geological Society [London], v. 171, no. 1, p. 1–4, https://doi.org/10.1144/jgs2013-020.

Reeve, M.T., Bell, R.E., Duffy, O.B., Jackson, C.A.L., and Sansom, E., 2015, The growth of non-colinear normal fault systems; what can we learn from 3-D seismic reflection data?: Journal of Structural Geology, v. 70, p. 141–155, https://doi.org/10.1016/j.jsg.2014.11.007.

Reston, T.J., 1996, The S reflector west of Galicia: The seismic signature of a detachment fault: Geophysical Journal International, v. 127, no. 1, p. 230–244, https://doi.org/10.1111/j.1365-246X.1996.tb01547.x.

Reston, T.J., 1988, Evidence for shear zones in the lower crust offshore Britain: Tectonics, v. 7, no. 5, p. 929–945, https://doi.org/10.1029/TC007i005p00929.

Reynisson, R.F., Ebbing, J., Lundin, E., and Osmundsen, P.T., 2010, Properties and distribution of lower crustal bodies on the mid-Norwegian margin, *in* Vining, B.A., and Pickering, S.C., eds., Petroleum Geology: From Mature Basins to New Frontiers—Proceedings of the 7th Petroleum Geology Conference: London, Geological Society, p. 843–854.

Ritzmann, O., and Faleide, J.I., 2007, Caledonian basement of the western Barents Sea: Tectonics, v. 26, TC5014, https://doi.org/10.1029/2006TC002059.

Roberts, A.M., Yielding, G., Kusznir, N.J., Walker, I.M., and Dorn-Lopez, D., 1995, Quantitative analysis of Triassic extension in the northern Viking graben: Journal of the Geological Society [London], v. 152, no. 1, p. 15–26, https://doi.org/10.1144/gsjgs.152.1.0015.

Roffeis, C., and Corfu, F., 2014, Caledonian nappes of southern Norway and their correlation with Sveconorwegian basement domains, *in* Corfu, F., Gasser, D., and Chew, D.M., eds., New Perspectives on the Caledonides of Scandinavia and Related Areas: Geological Society, London, Special Publication 390, p. 193–221, https://doi.org/10.1144/SP390.13.

Root, D.B., Hacker, B.R., Mattinson, J.M., and Wooden, J.L., 2004, Zircon geochronology and ca. 400 Ma exhumation of Norwegian ultrahigh-pressure rocks: An ion microprobe and chemical abrasion study: Earth and Planetary Science Letters, v. 228, no. 3, p. 325–341, https://doi.org/10.1016/j.epsl.2004.10.019.

Ruiz, M., Díaz, J., Pedreira, D., Gallart, J., and Pulgar, J.A., 2017, Crustal structure of the North Iberian continental margin from seismic refraction/wide-angle reflection profiles: Tectonophysics, v. 717, p. 65–82, https://doi.org/10.1016/j.tecto.2017.07.008.

Seranne, M., and Seguret, M., 1987, The Devonian basins of western Norway: Tectonics and kinematics of an extending crust, *in* Coward, M.P., Dewey, J.F., and Hancock, P.L., eds., Continental Extensional Tectonics: Geological Society, London, Special Publication 28, p. 537–48, https://doi.org/10.1144/GSL.SP.1987.028.01.35.

Shaocheng, J., Salisbury, M.H., and Hanmer, S., 1993, Petrofabric, P-wave anisotropy and seismic reflectivity of high-grade tectonites: Tectonophysics, v. 222, p. 195–226, https://doi.org/10.1016/0040-1951(93)90049-P.

Simancas, J.F., Carbonell, R., González Lodeiro, F., Pérez Estaún, A., Juhlin, C., Ayarza, P., Kashubin, A., Azor, A., Martínez Poyatos, D., Almodóvar, G.R., Pascual, E., Sáez, R., and Expósito, I., 2003, Crustal structure of the transpressional Variscan orogen of SW Iberia: SW Iberia Deep Seismic Reflection Profile (IBERSEIS): Tectonics, v. 22, 1062, https://doi.org/10.1029/2002TC001479.

Skilbrei, J.R., Kihle, O., Olesen, O., Gellein, J., Sindre, A., Solheim, D., and Nyland, B., 2000, Gravity Anomaly Map Norway and Adjacent Ocean Areas: Trondheim, Norway, Geological Survey of Norway, scale 1:3,000,000.

Skjerlie, F.J., 1985, Berggrunnskart Askvoll 1117 IV: Trondheim, Norges Geologiske Undersökelse, scale 1:50,000.

Slagstad, T., Barrére, C., Davidsen, B., and Ramstad, R.K., 2008, Petrophysical and thermal properties of pre-Devonian basement rocks on the Norwegian continental margin: Norges Geologiske Undersøkelse Bulletin, v. 448, p. 1–6.

Smethurst, M.A., 2000, Land-offshore tectonic links in western Norway and the northern North Sea: Journal of the Geological Society [London], v. 157, no. 4, p. 769–781, https://doi.org/10.1144/jgs.157.4.769.

Smithson, S.B., and Johnson, R.A., 2003, Petrological causes of seismic heterogeneity in the continental crust, *in* Goff, J.A., and Holliger, K., eds., Heterogeneity in the Crust and Upper Mantle: Nature, Scaling, and Seismic Properties: Berlin, Springer, p. 37–66.

Smithson, S.B., Wenzel, F., Ganchin, Y.V., and Morozov, I.B., 2000, Seismic results at Kola and KTB deep scientific boreholes: Velocities, reflections, fluids, and crustal composition: Tectonophysics, v. 329, p. 301–317, https://doi.org/10.1016/S0040-1951(00)00200-6.

Smythe, D.K., Dobinson, A., McQuillin, R., Brewer, J.A., Matthews, D.H., Blundell, D.J., and Kelk, B., 1982, Deep structure of the Scottish Caledonides revealed by the MOIST reflection profile: Nature, v. 299, p. 338–340, https://doi.org/10.1038/299338a0.

Snyder, D.B., 1990, The Moine thrust in the BIRPS data set: Journal of the Geological Society [London], v. 147, no. 1, p. 81–86, https://doi.org/10.1144/gsjgs.147.1.0081.

Sømme, T.O., Jackson, C.A.-L., and Vaksdal, M., 2013, Source-to-sink analysis of ancient sedimentary systems using a subsurface case study from the Møre-Trøndelag area of

southern Norway: Part 1—Depositional setting and fan evolution: Basin Research, v. 25, no. 5, p. 489–511, https://doi.org/10.1111/bre.12013.

Steel, R.J., 1976, Devonian basins of western Norway—Sedimentary response to tectonism and to varying tectonic context: Tectonophysics, v. 36, p. 207–224, https://doi.org/10.1016/0040-1951(76)90017-2.

Steel, R., and Aasheim, S.M., 1977, Alluvial sand deposition in a rapidly subsiding basin (Devonian, Norway), *in* Miall, A.D., ed., Fluvial Sedimentology: Canadian Society of Petroleum Geologists Memoir 5, p. 385–412.

Steel, R.J., Næhle, S., Nilsen, H., Røe, S.L., and Spinnangr, A., 1977, Coarsening-upward cycles in the alluvium of Hornelen Basin (Devonian) Norway: Sedimentary response to tectonic events: Geological Society of America Bulletin, v. 88, no. 8, p. 1124–1134, https://doi.org/10.1130/0016-7606(1977)88<1124:CCITAO>2.0.CO;2.

Stratford, W., and Thybo, H., 2011, Seismic structure and composition of the crust beneath the southern Scandes, Norway: Tectonophysics, v. 502, p. 364–382, https://doi.org/10.1016/j.tecto.2011.02.008.

Stratford, W., Thybo, H., Faleide, J.I., Olesen, O., and Tryggvason, A., 2009, New Moho map for onshore southern Norway: Geophysical Journal International, v. 178, no. 3, p. 1755–1765, https://doi.org/10.1111/j.1365-246X.2009.04240.x.

Sturt, B.A., and Braathen, A., 2001, Deformation and metamorphism of Devonian rocks in the Outer Solund area, western Norway: Implications for models of Devonian deformation: International Journal of Earth Sciences, v. 90, no. 2, p. 270–286, https://doi.org/10.1007/s005310000131.

Svensen, H., Jamtveit, B., Banks, D.A., and Karlsen, D., 2001, Fluids and halogens at the diagenetic–metamorphic boundary: Evidence from veins in continental basins, western Norway: Geofluids, v. 1, no. 1, p. 53–70, https://doi.org/10.1046/j.1468-8123.2001.11003.x.

Templeton, J.A., 2015, Structural Evolution of the Hornelen Basin (Devonian, Norway) from Detrital Thermochronology [Ph.D. thesis]: New York, Columbia University, 257 p., https://doi.org/10.7916/D87S7N9P.

Torsvik, T.H., Sturt, B.A., Ramsay, D.M., Kisch, H.J., and Bering, D., 1986, The tectonic implications of Solundian (Upper Devonian) magnetization of the Devonian rocks of Kvamshesten, western Norway: Earth and Planetary Science Letters, v. 80, p. 337–347, https://doi.org/10.1016/0012-821X(86)90115-9.

Torvela, T., Moreau, J., Butler, R. W., Korja, A., and Heikkinen, P., 2013, The mode of deformation in the orogenic mid-crust revealed by seismic attribute analysis: Geochemistry Geophysics Geosystems, v. 14, no. 4, p. 1069–1086, https://doi.org/10.1002/ggge.20050.

Varsek, J.L., and Cook, F.A., 1994, Three-dimensional crustal structure of the eastern Cordillera, southwestern Canada and northwestern United States: Geological Society of America Bulletin, v. 106, no. 6, p. 803–823, https://doi.org/10.1130/0016-7606(1994)106<0803:TDCSOT>2.3.CO;2.

Veludo, I., Dias, N.A., Fonseca, P.E., Matias, L., Carrilho, F., Haberland, C., and Villaseñor, A., 2017, Crustal seismic structure beneath Portugal and southern Galicia (western Iberia) and the role of Variscan inheritance: Tectonophysics, v. 717, p. 645–664, https://doi.org/10.1016/j.tecto.2017.08.018.

Vetti, V.V., 2008, Structural Development of the Håsteinen Devonian Massif, its Caledonian Substrate and the Subjacent Nordfjord–Sogn Detachment Zone—A Contribution to the Understanding of Caledonian Contraction and Devonian Extension in West Norway [Ph.D. thesis]: Bergen, Norway, University of Bergen, 481 p.

Vetti, V.V., and Fossen, H., 2012, Origin of contrasting Devonian supradetachment basin types in the Scandinavian Caledonides: Geology, v. 40, no. 6, p. 571–574, https://doi.org/10.1130/G32512.1.

Wain, A., 1997, New evidence for coesite in eclogite and gneisses: Defining an ultrahigh-pressure province in the Western Gneiss Region of Norway: Geology, v. 25, no. 10, p. 927–930, https://doi.org/10.1130/0091-7613(1997)025<0927:NEFCIE>2.3.CO;2.

Wang, C.-Y., Okaya, D.A., Ruppert, C., Davis, G.A., Guo, T.S., Zhong, Z., and Wenk, H.R., 1989, Seismic reflectivity of the Whipple Mountain shear zone in southern California: Journal of Geophysical Research–Solid Earth, v. 94, no. B3, p. 2989–3005, https://doi.org/10.1029/JB094iB03p02989.

Waters, C., Tikoff, B., Goodwin, L.B., and Little, T.A., 2003, Ductile instabilities and structural heterogeneity in the lower continental crust, *in* Goff, J.A., and Holliger, K., eds., Heterogeneity in the Crust and Upper Mantle: Berlin, Springer, p. 1–36.

Wilks, W.J., and Cuthbert, S.J., 1994, The evolution of the Hornelen Basin detachment system, western Norway: Implications for the style of late orogenic extension in the southern Scandinavian Caledonides: Tectonophysics, v. 238, p. 1–30, https://doi.org/10.1016/0040-1951(94)90047-7.

Wilson, R.W., Holdsworth, R.E., Wild, L.E., McCaffrey, K.J.W., England, R.W., Imber, J., and Strachan, R.A., 2010, Basement-influenced rifting and basin development: A reappraisal of post-Caledonian faulting patterns from the North Coast transfer zone, Scotland, *in* Law, R.D., Butler, R.W.H., Holdsworth, R.E., Krabbendam, M., and Strachan, R.A., eds., Continental Tectonics and Mountain Building: The Legacy of Peach and Horne: Geological Society, London, Special Publication 335, p. 795–826, https://doi.org/10.1144/SP335.32.

Yilmaz, O., 1987, Seismic Data Processing: Processing, Inversion, and Interpretation of Seismic Data, Volume 2: Society of Exploration Geophysicists Investigations in Geophysics 10, 2065 p., https://doi.org/10.1190/1.9781560801580.

Zhang, Z., Badal, J., Li, Y., Chen, Y., Yang, L., and Teng, J., 2005, Crust–upper mantle seismic velocity structure across southeastern China: Tectonophysics, v. 395, p. 137–157, https://doi.org/10.1016/j.tecto.2004.08.008.

Ziegler, P.A., 1975, Geologic evolution of North Sea and its tectonic framework: American Association of Petroleum Geologists Bulletin, v. 59, no. 7, p. 1073–1097.

MANUSCRIPT RECEIVED 11 APRIL 2017
REVISED MANUSCRIPT RECEIVED 26 OCTOBER 2018
MANUSCRIPT ACCEPTED 15 JANUARY 2019